# Elasticity and Hereditariness

**Luca Deseri**

**Abstract** This chapter collects the lecture notes of the module "Elasticity and Hereditatiness of Lipid Bilayers" delivered at CISM in July 2016. Such material is based primarily on three papers coauthored by this lecturer, and which have been contributing to shed light on the mechanical behavior of lipid bilayers. In particular, the breakthrough from this research is that the underlying nonlinear elastic response of lipid bilayers is fully determined as long as the membrane energy is obtained. Bending and saddle splay rigidities are shown here to be directly obtainable from the membranal response, as well as the line tension, holding together domains in which lipids are in different phases. The power law hereditariness of lipid membranes strikingly shown through rheometric tests has been analyzed in this work through a suitable energetics obtained by the author and coworkers and penalizing small perturbations of ground configurations of such systems.

L. Deseri (✉)
Department of Mechanical, Aerospace and Civil Engineering-MACE,
Brunel University London, Uxbridge UB8 3PH, UK
e-mail: luca.deseri@unitn.it; deseri.mems@pitt.edu

L. Deseri
Department of Mechanical Engineering and Materials Science-MEMS,
University of Pittsburgh, 636 Benedum Hall 3700 O'Hara Street, Pittsburgh, PA 15261, USA

L. Deseri
Department of Mechanical, Civil and Environmental Engineering-DICAM,
University of Trento, 38123 Trento, Italy

L. Deseri
Department of Mechanical Engineering, Carnegie Mellon University, Pittsburgh,
PA 15213-3890, USA

L. Deseri
Department of Nanomedicine, The Methodist Hospital Research Institute, MS B-490,
Houston, TX 77030, USA



D.J. Steigmann (ed.), *The Role of Mechanics in the Study of Lipid Bilayers*,
CISM International Centre for Mechanical Sciences 577,
DOI 10.1007/978-3-319-56348-0_2

## 1 Introduction

In Deseri et al. (2008) we obtained an energetics for biomembranes, such as lipid bilayers, which accounts for the through-thickness phase transition exhibited by planar structures and curved closed liposomes, like Giant Unilamellar Vescicles (GUVs) (see e.g., Lipowsky and Sackmann 1995). As pointed out in other chapters of this volume, the average thickness of such structures is of the order of 5 nm while the other two dimensions are several orders of magnitudes higher in size. In the treatment mentioned above no distinction is done between the leaflets of a bilayer, thereby inferring that even the energetics of lipid monolayers is compatible with such derivation.

Ways for controlling the morphologies in planar lipid systems and in GUVs are temperature and osmotic pressure based (see e.g., Baumgart et al. 2003; Veatch et al. 2004). Advanced high-resolution fluorescence imaging techniques employed in Baumgart et al. (2003) in particular have highlighted the coexistence of regions (or *phases*) with completely different features, highlighted in red and blue in Fig. 1 included in the same paper. The main contrast among such zones on the membranes is in terms of "degree of curliness" of the lipids, namely how curly and, hence, how short they get relative to their maximum length. This has an impact on the values of the curvatures in GUVs in regions with different degrees of curliness and also in the redistribution of the species within a lipid membrane with a given chemical composition. Because lipid membranes have the molecules free to move in-plane, namely across the surface, the two phases are called *liquid ordered-*$L_o$ and *liquid disordered-*$L_d$. In some cases, the presence of "lipid rafts" is detected in lipid bilayers. Basically, glycosphingolipid-enriched domains do form such rafts. For instance, the latter occur in the presence of fully saturated chains of sphingomyelin and glycosphingolipids bond with neighboring active functional glycosyl groups. Obviously, any model owing the $L_o$–$L_d$ transition can consistently predict lipid rafts. The issue is: can a model at the continuum level be more physically based and predict both the phase transitions and the changes in curvature and shapes? Through the last four decades this has been one of the main tasks in the field and, obviously, there no unique answer to this. Among the most prominent works in this direction

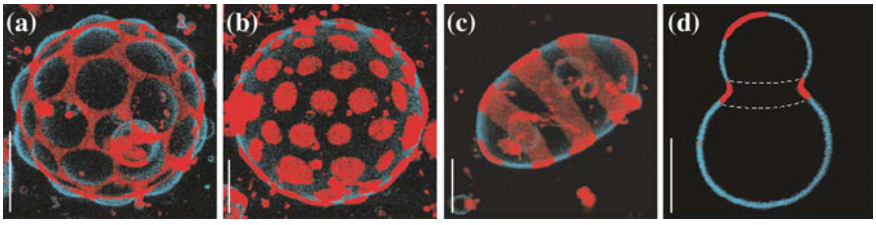


**Fig. 1** Images experimentally obtained by Baumgart et al. (2003), showing how phase separation relates to shapes achieved by GUVs. In *red* and *blue* respectively liquid-disordered and liquid-ordered phases. Scale bars 5 μm (Images by courtesy of Baumgart et al. 2003)

one can certainly single out Lipowsky and Sackmann (1995)-Chap. 1. There it was remarked that "here the theory of nonreacting mixtures and the theory of phase transitions are strictly related to the theory of thin, fluid shells". Ultimately, this corroborates the fact that obtaining a physically based model at the continuum level incorporating information regarding the species forming the bilayer, and rendering out the phase transition and the geometrical changes experienced by such structures is an extremely hard task. Contributions focusing on the purely mechanical behavior of such systems can be related to the pioneering work in Canham (1970), Fung (1966), Fung and Tong (1968), although the keystone work in biophysics regarding lipid bilayers can be singled out in Helfrich (1973), where the free energy density per unit area in the case of pure bending was obtained. This led the *Helfrich free energy*, which does coincide with the Kirchhoff–Love bending energy density in the presence of large curvature changes. The latter is well known in Structural Engineering and Solid Mechanics.

A piecewise Helfrich's energy has been employed when different zones of the surface of the bilayer are already known to be occupied by lipids in different phases. Spontaneous curvature in GUVs has also been accounted for in some of the extensions of Helfrich's model.

Along similar lines, a purely mechanical energy for liquid films has been obtained in Keller and Merchant (1991), where the bending stiffness of a liquid surface has been computed. Later, in Steigmann (1999) an expression of the dependence for two-dimensional fluid films exhibiting such stiffness was singled out, thanks to a theory of elastic surfaces. Along similar lines of thinking, in Baesu et al. (2004) it was proposed a stretching–bending energy density.

In all the models above the bilayer was always considered a two-dimensional body, thereby neglecting direct information associated with the thickness of the membrane. This is certainly not what one must do in order to capture the main mechanism of the observed phase transition experienced by the lipids. Indeed, they are seen to be nearly extended in the ordered phase, $L_o$, whereas they get shorter and curlier in the disordered phase, $L_d$. Indeed, it is known that a raise in temperature causes the hydrocarbon lipid tails of phospholipids to undergo the phase transition just mentioned above, evidenced by a significant thickness reduction from the liquid-ordered phase $L_o$ to the liquid-disordered phase $L_d$ (see e.g., Falkovitz et al. 1982; Goldstein and Leibler 1988, 1989; Jahnig 1981, 1996; Owicki et al. 1978; Owicki and McConnell 1979; Lipowsky and Sackmann 1995).

The conclusion is that keeping track of thickness changes is essential for lipid membranes and its changes witness the variations of the lipids order. This key issue is addressed in Deseri et al. (2008).

Asymptotic approaches delivering the mechanics of nonlinear elastic shells (see e.g., Koiter 1966) show that the thickness governs the scaling of both the membranal and the bending contributions to the energy density, being the former linear with the thickness while the latter is cubic in this quantity. Henceforth, ignoring the membranal term (as many formulations do) means to neglect an energy contribution to the overall energy which is two orders of magnitude more important than the bending term.

The work done in Deseri et al. (2008) also represents one of the first attempts toward a better understanding of the correlation among lipid order, membrane shape, and chemical composition during either temperature changes or osmotic pressure or both. This has been followed by several contributions in recent years, including Maleki et al. (2013). A related discussion and a derivation of the *line tension*, namely the configurational force arising at between zones of difference phases allowing for zones of finite size, is presented in Deseri and Zurlo (2013). This agrees with results obtained in Trejo and Ben Amar (2011).

The final reduced two-dimensional energetics in Deseri et al. (2008) is consistent with a dimension reduction procedure. This is done in two steps. The first one is to impose a modified Kirchhoff–Love kinematics which accounts for the thickness changes and by enforcing a new symmetry group, introduced in Zurlo (2006), proved Healey et al. (2017) and, eventually in Maleki et al. (2013), thereby delivering a bulk energy density as a function of solely three invariants of the Cauchy–Green strain measure. The second step is to perform an asymptotic expansion of the bulk energy with respect to a reference thickness.

Summing up, the resulting energy density confirms the hierarchy between the membranal and the bending terms described above, although it delivers a uniquely and strikingly revealing expression, explained in Sect. 2. This will eventually lead to deducing the key features of the elastic part of the response of lipid membranes, such as the areal and bending rigidities and the line tension, namely the configurational force holding together zones in different phases.

The main feature of the energy derived in Deseri et al. (2008) is the presence of two turning points in the local stress governing the biological membrane behavior (see Fig. 7a). They are placed in the spinoidal zone for the local part of the energy. Henceforth, whenever the external conditions are such that the aerial stretch, i.e., the reciprocal of the thinning, is enclosed in this region, the response may produce a rapid change of the geometry, i.e., material instabilities can occur. The onset of bifurcated configurations possibly arising from homogeneous configurations characterized by an areal stretch lying in the spinoidal region is studied in Sect. 2.5. The total elastic (Gibbs free) energy expanded upon any ground state in such region will be studied to determine the bifurcated modes and the relationships between the number of nucleated spatial oscillations with the critical values of the areal stretches.

In the sequel we will show that this occurrence is exhibited even when the in-plane viscosity of the lipid membrane is accounted for. In this regard, the experimental observations of lipid viscous behavior showed that the loss and storage moduli are well described by power law functions (Espinosa et al. 2011). This observation suggests that the behavior of the biological membrane is properly described in the framework of fractional hereditariness.

An analysis of the appropriate energetics arising because of viscosity will lead to a new governing functional for studying the influence of the effective viscoelasticity of the lipid membrane on the material instabilities exhibited by the system which is studied in Sect. 3. The resulting viscoelastic free energy has a local and a nonlocal part. There, the power at which stress and hyperstress relax might be different, as

diffusion mechanisms may occur at different average speeds depending on whether or not they arise in a boundary layer between different phases or in a given phase.

Exactly like in the purely elastic case, values of the areal stretches for which unknown time evolving bifurcated configurations could occur are sought. This is to investigate the role of the hereditariness on such unstable ground states. To this aim, in full analogy with the elastic case, a variational principle is employed. The Gibbs free energy density prevailing the space-time varying perturbation is taken from Deseri et al. (2014), where a hierarchical rheological model yields the Staverman–Schartzl free energy (extensively studied in Del Piero and Deseri 1996, 1997; Deseri et al. 2006, among many others) as the one for power law materials.

The variational principle yields a non-classical eigenvalue problem. Spatial modes bifurcating from ground states characterized by the areal stretch within the spinoidal zone are of course oscillatory. The period of spatial oscillation is shown to decrease with the ratio of generalized local and nonlocal moduli. Henceforth, the number of oscillations increases with respect to the elastic case. As the ratio just mentioned above increases, for a given number of oscillations the interval of stretches for which bifurcation can occur gets larger if compared with the one determined by the purely elastic behavior. The model then is suggesting that hereditariness increases the chances of nucleating spatially oscillatory bifurcated modes.

Upon exploring the transfer function of the equation governing the eigenvalue problem mentioned above, it is found that, for various values of the local and nonlocal relaxation power, time decay occurs in the response. Hence, spatial oscillations do slowly relax, exhibiting a long tail type response in time.

## 2 The New Elastic Energy for Lipid Membranes

In this section we briefly recall the main results obtained in Deseri et al. (2008), together with a schematic description of the approach followed in this work. The main result is the derivation of a new surface energy density for the lipid bilayer. This is shown to give the possibility of deducing bending rigidities, line tension, and thickness profile inside the boundary layer during the order–disorder transition from simple experimental data on the stretching behavior of the membrane.

Attention here will be restricted to initially planar membranes, thereby neglecting the effects of spontaneous curvature. An orthonormal basis $(\boldsymbol{e}_1, \boldsymbol{e}_2, \boldsymbol{e}_3)$ is introduced to describe material points in the reference configuration and geometrical changes with respect to that. A simply connected region $\mathscr{B}_0$ of constant thickness $h_0$ in the direction of $\boldsymbol{e}_3$ and with a flat mid-surface $\Omega$ in the plane spanned by $(\boldsymbol{e}_1, \boldsymbol{e}_2)$ depicts the reference configuration for the membrane, thereby not distinguishing between the upper and the lower leaflet of the membrane. Points of $\mathscr{B}_0$ are denoted by

$$\boldsymbol{x} = \mathbf{x} + z\boldsymbol{e}_3,$$

where

$$\mathbf{x} = x\boldsymbol{e}_1 + y\boldsymbol{e}_2$$

and $z \in (-h_0/2, h_0/2)$.

In the sequel $\boldsymbol{f}$ represents the deformation map of $\mathscr{B}_0$ and $\mathbf{F} = \nabla \boldsymbol{f}$ its $3 \times 3$ gradient. The energy $\mathscr{E}$ stored in the membrane is symbolically expressed as follows:

$$\mathscr{E} = \int_{\mathscr{B}_0} W(\mathbf{F})\, dV = \int_{\Omega} \int_{-h_0/2}^{h_0/2} W(\mathbf{F})\, dz\, d\Omega, \tag{1}$$

where $W$ is the purely elastic Helmholtz energy density per unit volume. Evidently, the energy density per unit surface in the reference configuration reads as follows:

$$\psi = \int_{-h_0/2}^{h_0/2} W(\mathbf{F})\, dz. \tag{2}$$

In-plane fluidity is the main features of lipid membranes at room-to-body temperature. This entails the impossibility of sustaining shear stresses in planes perpendicular to $\boldsymbol{e}_3$, unless viscosity is accounted for. This has been used to restrict the dependence of $W$ on three suitable invariants of $\mathbf{F}$ (see Zurlo 2006; Healey et al. 2017 and Maleki et al. 2013), namely

$$\mathscr{I}(\boldsymbol{x}) = \{\bar{J}(\boldsymbol{x}), \det \mathbf{F}(\boldsymbol{x}), \bar{\phi}(\boldsymbol{x})\}, \tag{3}$$

representing the areal stretch of planes perpendicular to the direction $\boldsymbol{e}_3$, the volume change and the stretch across the thickness, which ultimately will deliver the order parameter for the degree of curliness of the lipids, respectively.

With the aim of catching the out-of-plane kinematics as well as thickness changes, the following ansatz is assumed for the 3D deformation (see Fig. 2):

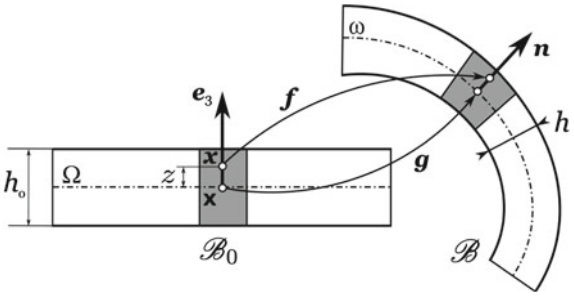


**Fig. 2** Schematic representation of the deformation (4) of a plate-like reference configuration $\mathscr{B}_0$ into the current configuration $\mathscr{B}$. The gray box depicts the space occupied by two lipid molecules, their volume being conserved during the deformation (courtesy of Deseri and Zurlo 2013)

$$\boldsymbol{f}(\boldsymbol{x}) = \boldsymbol{g}(\mathbf{x}) + z\,\phi(\mathbf{x})\boldsymbol{n}(\mathbf{x}), \tag{4}$$

where $\boldsymbol{g}(\mathbf{x}) = \boldsymbol{g}(x, y, 0)$ defines the current mid-surface of the membrane, that is $\omega = \boldsymbol{g}(\Omega)$, where $\boldsymbol{n}$ is the outward normal to $\omega$ and where

$$\phi(\mathbf{x}) = h(\mathbf{x})/h_0$$

is the *thickness stretch*, with $h$ the current thickness. Such ansatz permits to make explicit the dependence of the invariants $\mathscr{I}$ on $z$ and, ultimately, to perform the expansion of (2) in powers of the reference thickness $h_0$.

The molecular volume of biological membranes can be shown to stay almost constant in a broad range of temperature (see e.g., Goldstein and Leibler 1989; Owicki et al. 1978). This condition can be made explicit through a *quasi-incompressibility* constraint, namely

$$\det \mathbf{F}(\mathbf{x}, 0) = \bar{J}(\mathbf{x}, 0)\phi(\mathbf{x}) = 1. \tag{5}$$

The gray area in Fig. 2 relates with neighboring lipid molecules across the upper and lower leaflets with respect to the film mid-surface. The constraint (5) is actually a first-order approximation of the exact incompressibility constraint, as $\det \mathbf{F}(\boldsymbol{x}) = \det \mathbf{F}(\mathbf{x}, 0) + O(z)$. In all planar deformations, namely whenever $\omega$ deforms in the plane $z = 0$, (5) yields that $\det \mathbf{F}(\boldsymbol{x}) = 1$ is exact. This is the special case considered in the sequel, thereby focusing on planar lipid membranes. It is not difficult to show that the 3D energy density $W$ reduces as follows:

$$w(J) = W(\bar{J}, \det \mathbf{F}, \bar{\phi})\Big|_{z=0} = W(J, 1, J^{-1}), \tag{6}$$

where

$$J(\mathbf{x}) = \bar{J}(\mathbf{x}, 0).$$

The ansatz (4) and the assumption of in-plane fluidity yield the following expansion of (2) up to terms of order $h_0^3$:

$$\psi = \varphi(J) + \kappa(J)H^2 + \kappa_g(J)K + \alpha(J)||\mathrm{grad}_\omega \widehat{J}||^2, \tag{7}$$

where $H$ and $K$ are, respectively, the mean and Gaussian curvatures of the mid-surface $\omega$, where

$$\varphi(J) = h_0\ w(J) \tag{8}$$

is the stretching energy density of the membrane, scaling with $h_0$, and where bending rigidities are found to be the following:

$$k(J) = \frac{h_0^2}{6}\varphi''(J) = \frac{h_0^3}{6}w''(J), \qquad k_G(J) = \frac{h_0^2}{12J}\varphi'(J) = \frac{h_0^3}{12J}w'(J), \tag{9}$$

where $' = d/dJ$. It is worth emphasizing that the latter scale with $h_0^3$, as expected. The last term in (7) reads as follows:

$$\alpha(J) = \frac{h_0^2}{24J^3}\varphi'(J), \tag{10}$$

and it penalizes the gradients of $J = h/h_0$, namely the presence of boundary layers between zones where the lipids are in either of the two possible phases. It is worth emphasizing that $\widehat{J}$ represents the spatial description $\widehat{J} \circ \boldsymbol{g} = J$ of $J$, and $\text{grad}_\omega$ is the spatial gradient, with respect to points of the current mid-surface $\omega$.

Often times the bending energy is calculated relative to the current surface $\omega$ and, hence, bending rigidities must be expressed relative to the same configuration (see e.g., Baumgart et al. 2003), i.e.,

$$\kappa(J) = \frac{h_0^2}{6J}\varphi''(J), \qquad \kappa_G(J) = \frac{h_0^2}{12J^2}\varphi'(J). \tag{11}$$

The expression (7) is consistent with several models previously introduced in the literature of biological membranes. Indeed, Helfrich's model

$$\psi = kH^2 + k_G K$$

is recovered whenever one considers fixed value of $J$ fixed.

The new energy (7) enables one to predict thickness phase transitions even for planar lipid membranes, including Langmuir films, that remain flat under external inputs, like temperature changes. Such situations are retrieved by (7) by setting $H = K = 0$. This energetics reminds of the resulting energy for cold drawing of polymeric films obtained in (see e.g., Coleman and Newman 1988). If the term factoring $\alpha$ is neglected, (7) agrees with the one determined in Baesu et al. 2004.

It is worth noting that the strategy followed in Deseri et al. (2008) and Zurlo (2006) to deliver (7) accounts for fairly general constitutive assumptions on the 3D energy $W$, and also accounts for chemical composition, temperature dependence and, potentially, for the presence of spontaneous curvature.

## *2.1 Stretching Energy*

As it is clear from the structure of (7) and from (11) and (10), the pivot information governing the whole energetics is the surface Helmholtz energy $\varphi(J)$. This regulates the in-plane stretching behavior of the membrane and allows for predicting the phase transition phenomena observed in lipid membranes (Fig. 3).

The experimental evidence clearly shows that for a given chemical composition there may exist a temperature range where the $L_o$ and $L_d$ phases coexist, organizing themselves in domains called rafts. In closed membranes, these domains are

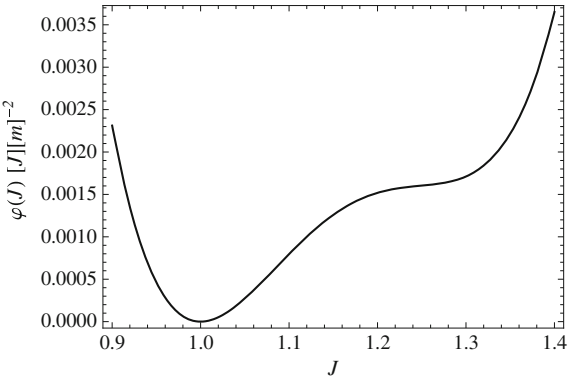


**Fig. 3** The stretching energy $\varphi(J)$ adapted from Goldstein and Leibler (1989), for a temperature $T \sim 30°$. The areal stretch $J_o = 1$ corresponds to the unstressed, reference configuration $\mathscr{B}_0$ (courtesy of Deseri and Zurlo 2013)

typically detectable by curvature inhomogeneities, reflecting the occurrence of different bending rigidities (Baumgart et al. 2003). The expressions (11) for the bending moduli enlighten how the order–disorder transition, described by the stretching energy $\varphi(J)$, is connected with bending behavior of the membrane. Furthermore, we will prove that the knowledge of $\varphi(J)$ also determines the line tension occurring at the phase boundary.

Several works, such as Falkovitz et al. (1982), Goldstein and Leibler (1989), Komura et al. (2004), Owicki et al. (1978), Owicki and McConnell (1979), show that in order to provide a suitable expression for $\varphi(J)$ a Landau expansion in terms of the powers of either the thinning field $\phi = h/h_0$ or the areal stretch $J$ is provided. This has the advantage that its (temperature dependent) coefficients are connected to the latent heat and the order parameter jump (e.g., Goldstein and Leibler 1989 and Lipowsky and Sackmann 1995). For the sake of convenience, in the sequel we assume that the natural planar configuration $\mathscr{B}_0$ of the lipid membrane is precisely the ordered phase $L_o$, where $J = J_o = 1$, so that the stretching energy takes the form

$$\varphi(J) = a_0 + a_1 J + a_2 J^2 + a_3 J^3 + a_4 J^4, \tag{12}$$

where the coefficients $a_i$ $(i = 0, \ldots, 4)$ depend on temperature and chemical composition. Lacking of more experimental information leads one to tune such parameters, thanks to experimentals provided in Goldstein and Leibler (1989), actually also utilized in Komura et al. (2004), to connect with the thinning transition experienced by the lipids. At room temperature $T \sim 30°$, one record the following coefficients for $\varphi(J)$:

$$\begin{gathered} a_0 = 2.03, \quad a_1 = -7.1, \quad a_2 = 9.23, \\ a_3 = -5.3, \quad a_4 = 1.13. \end{gathered} \tag{13}$$

It is worth noting that their dimension is $[J][m]^{-2}$. The choice (13) has been pursued with the aim to show the feasibility of the proposed treatment. Specific data on the bilayer chemical composition and the temperature are required in order to get realistic pictures of the geometrical changes during the expected phase transition.

Summing up we conclude that:

- the membrane energy density $\varphi(J)$ can be completely determined experimentally: this is a local term within the energy and depends on temperature, chemical composition (of the specific lipids), and it scales with the linear power of the reference thickness of the bilayer;
- bending and spatial changes of either the thickness change gradient or of the related areal stretch are detected by the energy, thanks to the arising nonlocal terms;
- the latter coincides with the Helfrich's energy when the gradient term is negligible with respect to the bending one and the elastic moduli do not significantly change with areal stretch and concentration;
- like in the case of Coleman and Newman (1988), the penalization of the gradient of the areal stretch spontaneously arises from the dimension reduction procedure;
- besides prescribing the mean and the Gaussian curvatures, the resulting bending energy density is completely determined by the sole membrane energy density $\varphi(J)$: this relates to the chemical composition of the membrane is the only needed constitutive information of the model.

## 2.2 Thinning Transition in Flat Lipid Layers

A planar membrane in the reference configuration $\mathscr{B}_0$ is displayed in Fig. 4. Its homogeneous thickness in the direction of $\boldsymbol{e}_3$ is denoted by $h_0$, while its width in the direction of $\boldsymbol{e}_2$ is labeled by $B$ and its length is denoted by $L$. At $z = 0$ the reference mid-surface $\Omega$ is set, while the sides of the planar bilayer are situated $x = \pm L/2$ and $y = \pm B/2$.

Plane strain deformations are considered to explore the main features of the thinning phase transition. Hence, the kinematics reads as follows:

$$\varphi(\boldsymbol{x}) = g(x)\boldsymbol{e}_1 + y\boldsymbol{e}_2 + z\phi(x)\boldsymbol{e}_3, \tag{14}$$

where $x$ is the variable in the direction $\boldsymbol{e}_1$. The deformation gradient of such $\varphi$ reads as follows:

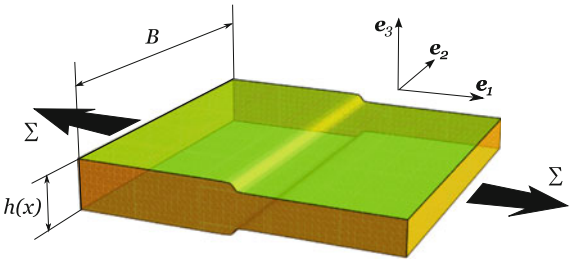


**Fig. 4** Plane strain lipid bilayer undergoing phase transition from the thicker $L_o$ domain to the thinner $L_d$ domain under a traction $\Sigma$ in the $\boldsymbol{e}_1$ direction (courtesy of Deseri and Zurlo 2013)

$$\mathbf{F} = \nabla\varphi = \begin{bmatrix} g_x & 0 & 0 \\ 0 & 1 & 0 \\ z\phi_x & 0 & \phi \end{bmatrix}, \tag{15}$$

where $_x$ denotes differentiation with respect to that (only) variable. The displacement component along $\boldsymbol{e}_1$ is $u(x) = g(x) - x$. The stretch in direction of the length of the bilayer is introduced in the sequel

$$\lambda(x) = g_x(x). \tag{16}$$

The 3D quasi-incompressibility reduces to $\phi = \lambda^{-1}$ on $\Omega$, so that the membrane deformation is completely determined by $\lambda$.

We note that

$$||\mathrm{grad}_\omega \hat{J}||^2 = ||\mathrm{grad}_\omega \hat{\lambda}||^2 = \lambda_x^2 \lambda^{-2}, \tag{17}$$

after setting $\hat{\lambda} = \lambda \circ g^{-1}$, representing the spatial description of $\lambda$,

The resulting energy density per unit area (7) reads as follows:

$$\psi(\lambda, \lambda_x) = \varphi(\lambda) + \frac{h_0^2}{24}\lambda^{-5}\varphi'(\lambda)\lambda_x^2 \tag{18}$$

where $' = d/d\lambda$ (here $J = \lambda$). Upon introducing

$$\gamma(\lambda) = -\frac{h_0^2}{12}\lambda^{-5}\varphi'(\lambda), \quad \beta(\lambda) = \frac{1}{2}\gamma'(\lambda), \tag{19}$$

(see Coleman and Newman 1988), the energy density above can be rewritten as follows:

$$\psi(\lambda, \lambda_x) = \varphi(\lambda) - \frac{1}{2}\gamma(\lambda)\lambda_x^2. \tag{20}$$

It is worth noting that if $\gamma$ would be replaced by a negative constant, the energy (20) coincides to the Cahn–Hilliard functional (Cahn and Hilliard 1958). The fact that the constant $\gamma < 0$ in such a model is required for stability purposes. In (19) the fact that $\gamma$ depends on $\lambda$ makes (20) to resemble the energy density deduced in Coleman and Newman (1988). Even in this case the condition $\gamma(\lambda) < 0$ is required for nucleating phase boundaries. This is in fact the case for the energy density (12).

For the sake of argument, opposite tractions $\Sigma$ (force per reference length) are taken to arise on the edges $x = \pm L/2$. Due to the presence of $\lambda_x$ hypertractions $\Gamma$ performing work against $u_x$ must be accounted for. Henceforth, the work performed on the bar reads as follows:

$$\mathscr{W}(u, u_x) = B\,[\Sigma u]_{-L/2}^{+L/2} + B\,[\Gamma u_x]_{-L/2}^{+L/2}. \tag{21}$$

Evidently, the total potential energy for any $g$ is the sum of the total strain energy, obtained by integrating (20) across the membrane, minus the work (21), i.e.,

$$\mathscr{E}(\gamma) = B \int_{-L/2}^{L/2} \psi(\lambda, \lambda_x)\, dx - \mathscr{W}(u, u_x). \tag{22}$$

Stationarity of (22) yields the Euler–Lagrange equation for $u$ and the associated boundary conditions. A perturbation $\eta(x)$ is imposed on the underlying $g$, namely

$$g_\varepsilon(x) := g(x) + \varepsilon\eta(x), \tag{23}$$

to deliver those information from (22). The arbitrariness of $\eta$ leads to the first variation $\delta E = dE(g_\varepsilon)/d\varepsilon|_{\varepsilon=0}$ of (22), thereby delivering the Euler–Lagrange equation. Upon integrating such relation, the following condition is obtained:

$$\Sigma = \varphi'(\lambda) + \beta(\lambda)\lambda_x^2 + \gamma(\lambda)\lambda_{xx} = const., \tag{24}$$

holding in the open interval $(-L/2, L/2)$, with the boundary conditions

$$[\Gamma + \gamma(\lambda)\lambda_x]_{-L/2} = [\Gamma + \gamma(\lambda)\lambda_x]_{+L/2} = 0. \tag{25}$$

Strain localizations are investigated to explore the possible coexistence of ordered regions, in the $L_o$ phase, and disordered zones, the thinner $L_d$ phase: this transition may be connected through a boundary layer. With the aim of getting rid of edge effects induced by the boundary (Coleman and Newman 1988), the length $L$ is considered unbounded relative to the reference thickness $h_0$. Henceforth, $-\infty < x < \infty$. The particular case in which $\Gamma = 0$ at the boundaries is explored in the sequel, so that (25) implies $\lambda_x \to 0$ as $x \to \pm\infty$. Nontrivial and bounded solutions of (24) are sought. In Coleman and Newman (1988) it is shown that they verify the equation

$$x - \bar{x} = \int_{\lambda(\bar{x})}^{\lambda(x)} \left( \frac{-2}{\gamma(\lambda)} \int_{\lambda_a}^{\lambda} \left[\varphi'(\zeta) - \Sigma\right] d\zeta \right)^{-\frac{1}{2}} d\lambda, \tag{26}$$

where $\bar{x}$ is arbitrary and where $\lambda_a$ is either the value of $\lambda$ at a specific location or a limiting value at which $\lambda_x = 0$. The derivation of (26) is detailed in Deseri and Zurlo (2013).

Whenever $\gamma(\lambda) < 0$, nontrivial bounded solutions of (24) have been completely characterized in Coleman and Newman (1988) for given tractions $\Sigma$. Depending on the number of locations at which $\lambda_x = 0$, the solutions of the problem are shown to fall in one of the following classes:

1. $\lambda$ is strictly monotone, if $\lambda_x \neq 0$ for any finite location;
2. $\lambda$ exhibits either a bulge or a neck, if there exists precisely one location $x$ at which $\lambda_x = 0$;
3. $\lambda$ is periodic, if there is more than one finite value of $x$ at which $\lambda_x = 0$.

Strictly monotone solutions are analyzed in the sequel. In such cases the following relations hold:

$$\begin{array}{ll} \lim_{x\to-\infty}\lambda=\lambda_*, & \lim_{x\to+\infty}\lambda=\lambda^* \\ \lim_{x\to\pm\infty}\lambda_x=0, & \lim_{x\to\pm\infty}\lambda_{xx}=0. \end{array} \tag{27}$$

Coleman and Newman (1988) show that such conditions can be attained provided that the applied traction equals the Maxwell stress $\Sigma_M$, which is determined by the equal area rule

$$\int_{\lambda_*}^{\lambda^*}[\varphi'(\lambda)-\Sigma_M]\,d\lambda=0, \tag{28}$$

with

$$\varphi'(\lambda_*)=\varphi'(\lambda^*)=\Sigma_M,$$

bearing in mind that these solutions are uniquely determined to within a reflection or translation. The fact that $\lambda(x)$ is monotonic allows for determining the location map $x$ in terms of $\lambda$ from (26), with $\lambda_a\equiv\lambda_*$ and $\bar{x}$ arbitrary, such that $\lambda_*<\lambda(\bar{x})<\lambda^*$.

For the specific energy (12), it turns out that

$$\Sigma_M=5.92\,\mathrm{mN\,m^{-1}},\quad \lambda_*=1.025,\quad \lambda^*=1.308, \tag{29}$$

which is consistent with what it is displayed in (see Fig. 5). For the sake of illustration, one may take $h_0=45.5$ Å for the reference thickness of the ordered phase (see Deseri and Zurlo 2013) and its reference to Goldstein and Leibler (1989) and by making use of (12, 19), the numerical integration of (26) yields $\lambda(x)$ within the range $(\lambda_*,\lambda^*)$.

The boundary layer is displayed in Fig. 6 as a result of the solutions of the Euler–Lagrange equation mentioned above. Evidently, with $\lambda(x)$ strictly monotonic, the limit values $(\lambda_*,\lambda^*)$ are asymptotic values at infinity. Nonetheless, the solution depicted in Fig. 6 is characterized by a strong strain localization inside a boundary layer of length $\simeq$15 Å. It is between $\lambda_*$ and $\lambda^*$ where such a boundary layer is almost completely localized. As it was expected, the length of the boundary layer and the membrane thickness are of the same order. This is in agreement with

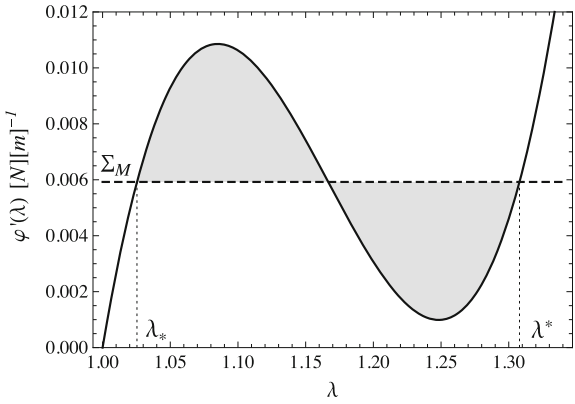


**Fig. 5** The function $\varphi'(J)$ and the value of the Maxwell stress $\Sigma_M=5.92\,\mathrm{mN\,m^{-1}}$, resulting from the equal area construction (*gray regions*) (courtesy of Deseri and Zurlo 2013)

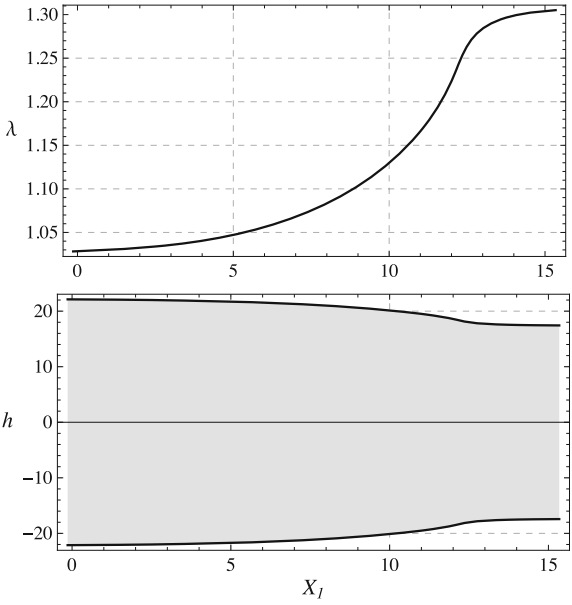


**Fig. 6** The function $\lambda(x)$ (*up*) and the thickness profile $h(x)$ (*down*) in correspondence of $\Sigma = \Sigma_M$. Lengths expressed in Å (courtesy of Deseri and Zurlo 2013)

previously obtained estimates, such as the one obtained in Akimov et al. (2004). It goes without saying that the stretch is almost constant outside the boundary layer. The two domains where the stretch is practically equal to $\lambda_*$ and $\lambda^*$ are the $L_o$ and $L_d$ phases, respectively. From (24), the (Piola) stress (per reference length) in both phases equals $\Sigma_M$, whereas the Cauchy stress (per current length) in the two domains amounts to

$$\begin{aligned} t^{L_o} &= t_* = \Sigma_M \lambda_* = 6.07\,\mathrm{mN\,m^{-1}} \\ t^{L_d} &= t^* = \Sigma_M \lambda^* = 7.74\,\mathrm{mN\,m^{-1}}. \end{aligned} \tag{30}$$

Of course such values strongly depend on the form of $\varphi(J)$ taken in (12). Although this is certainly the case, such values are consistent with estimates of surface stress in ordered and disordered domains inferred through experimental investigations (see e.g., Semrau et al. 2008). In the latter paper it is shown that the stress in the disordered phase is significantly higher than in the ordered one. Furthermore, the values of surface stress obtained in this analysis are within the range of values of tension physiologically intrinsic of lipid membranes, namely ($0-15\,\mathrm{mN\,m^{-1}}$). The estimates above agree with the results in Reddy et al. (2012), where the role played by surface tension in changes of the lipid conformational order has been investigated.

## 2.3 *Line Tension Holding Zones in a Given Phase*

Before introducing the line tension, as the configurational force capable to hold zones in one phase surrounded by others in a different phase, we prove that (26) is a global

minimizer of the total potential energy $\mathscr{E}$ in the class of smooth solutions fulfilling the boundary conditions (27). Furthermore, one can also show that this profile delivers an optimal value of the line tension.

In order to do so, we recall that phase coexistence follows two different approaches: the gradient theory and the sharp interface approximation.

The gradient theory does not allow discontinuities in the field. In either case, the analysis leading to phase transition between two different zones relies upon minimizing the total potential energy introduced earlier in the text, namely:

$$\mathscr{E} = \int_\Omega \left[\varphi(J) + \alpha(J)||\mathrm{grad}_\omega \hat{J}||^2\right] d\Omega - \mathscr{W}. \tag{31}$$

The sharp interface approximation allows for the order parameter $J$ to be subject to discontinuities; in this case the total potential energy reads

$$\mathscr{F} = \int_\Omega \varphi(J)\, d\Omega + \sigma\, \ell([\![J]\!]) - \mathscr{W}, \tag{32}$$

where $\sigma$ is the *line tension* between the two phases which, from the dimensional standpoint, is a force. Here $\ell$ is the length of the interface, which in this approximation is a jump set, i.e., the union of regions across which $J$ can tolerate jumps.

In Deseri and Zurlo (2013) a rigorous analysis demonstrates the strict connection between the sharp interface approach and the gradient theory. Indeed, it is proved that minimizers of $\mathscr{E}$ converge (in a suitable sense) to minimizers of $\mathscr{F}$ (see e.g., Alberti 2000 for explanations). An optimal value for the line tension can be deduced by evaluating the global minima of $\mathscr{E}$ in the class of solutions fulfilling the boundary conditions (27).

Because of compatibility we recall that $u_x(x) = \lambda(x) - 1$. Henceforth, the work can be rewritten as follows:

$$\mathscr{W} = B \int_{-L/2}^{L/2} \Sigma_M \lambda\, dx - B\Sigma_M L. \tag{33}$$

It is worth noting that the following quantity, essentially representing a Gibbs free energy density for the lipid membrane, remains constant at the minimizer, i.e.,

$$\varphi(\lambda_*) - \Sigma_M \lambda_* = \varphi(\lambda^*) - \Sigma_M \lambda^*.$$

This suggests to consider the energy

$$\tilde{\varphi}(\lambda) = \varphi(\lambda) + c,$$

where

$$c = \Sigma_M \lambda_* - \varphi(\lambda_*) = \Sigma_M \lambda^* - \varphi(\lambda^*), \tag{34}$$

so that

$$\tilde{\varphi}(\lambda_*) - \Sigma_M \lambda_* = \tilde{\varphi}(\lambda^*) - \Sigma_M \lambda^* = 0. \tag{35}$$

We also note that away from the characteristic stretches $\lambda_*$ and $\lambda^*$, i.e., for $\lambda \neq \lambda_*$ and $\lambda \neq \lambda^*$, the following inequality holds:

$$\tilde{\varphi}(\lambda) - \Sigma_M \lambda \geq 0. \tag{36}$$

After discussing the sharp interface approximation, the gradient functional is now analyzed. Outcomes from the latter will be compared with the former. Indeed the film is subject to a traction $\Sigma_M$, and we consider a monotonic stretch profile $\lambda(x)$ within the interval $(-L/2, L/2)$. Assume that $\lambda \to \lambda_*$ as $x \to -L/2$ and that $\lambda \to \lambda^*$ as $x \to L/2$. Obviously, $\Sigma_M$ is the Maxwell value introduced in Sect. 2.2.

Consider the total potential energy per unit length $\mathscr{E}/L$. By utilizing ((33), (35)), for any thickness profile satisfying the boundary conditions (27), the relation below follows:

$$\frac{\mathscr{E}}{L} = \frac{B}{L} \int_{-L/2}^{L/2} \left[ (\tilde{\varphi}(\lambda) - \Sigma_M \lambda) - \frac{\gamma(\lambda)}{2} \lambda_x^2 \right] dx + d, \tag{37}$$

where $d = B(\Sigma_M - c)$ is a constant.

On closing, the profile characterized by (26) and verifying stationarity is now shown to be a minimizer for $\mathscr{E}/L$. This is based on a result in Alberti (2000). By $\tilde{\varphi}(\lambda) - \Sigma_M \lambda \geq 0$, by $-\gamma(\lambda)\lambda_x^2 \geq 0$, by the monotonicity of $\lambda$ and by the inequality $a^2 + b^2 \geq 2ab$, it follows the following inequality:

$$\frac{\mathscr{E}}{L} \geq \frac{B}{L} \int_{\lambda_*}^{\lambda^*} \sqrt{-2\gamma(\lambda)\,(\tilde{\varphi}(\lambda) - \Sigma_M \lambda)}\; d\lambda + d, \tag{38}$$

and equality holds if and only if $a = b$, namely if and only if

$$\tilde{\varphi}(\lambda) - \Sigma_M \lambda = -\frac{\gamma(\lambda)}{2} \lambda_x^2. \tag{39}$$

If one now simply recognizes that

$$\tilde{\varphi}(\lambda) - \Sigma_M \lambda = \int_{\lambda_*}^{\lambda} \left( \varphi'(\zeta) - \Sigma_M \right) d\zeta \tag{40}$$

from (35), (26) is obtained in exact form by integrating (39). Finally, we just showed that the following minimum is actually attained:

$$\begin{aligned} &\min \left( \frac{\mathscr{E}}{L} \right) = \\ &= \frac{B}{L} \int_{\lambda_*}^{\lambda^*} \sqrt{-2\gamma(\lambda)\,(\tilde{\varphi}(\lambda) - \Sigma_M \lambda)}\; d\lambda + d, \end{aligned} \tag{41}$$

within the functions verifying the boundary conditions (27), provided that $\lambda(x)$ is given by (26).

Consider now any configuration characterized by $\lambda = \lambda_*$ for $x < x_0$ and $\lambda = \lambda^*$ for $x > x_0$, so that in $x = x_0$ there is a sharp interface. The location $x_0$ is an arbitrary finite point. In this configuration, one can show that the total potential energy per unit length (32) becomes

$$\frac{\mathscr{F}}{L} = \frac{B}{L}\sigma + d. \tag{42}$$

By comparing (37), (41) and (42) the line tension of the sharp interface model remains determined as follows:

$$\sigma = \int_{\lambda_*}^{\lambda^*} \sqrt{-2\gamma(\lambda)\,(\tilde{\varphi}(\lambda) - \Sigma_M \lambda)}\; d\lambda. \tag{43}$$

Numerical data (13) and integration of (43) owe the following number for the line tension:

$$\sigma = 3.88 \cdot 10^{-13}\mathrm{N} \tag{44}$$

which is consistent with the experimentally found value $9 \pm 0.3 \cdot 10^{-13}$N (see e.g., Baumgart et al. 2003; Semrau et al. 2008). The predicted thickness profile and line tension are then consistent with pre-existing analyses for lipid membranes, that account for the competition of stretching and tilt elasticity. This latter phenomenon is due to the fact that lipid molecules can deviate from the mid-surface normal (see e.g., Akimov et al. 2004; Hamm and Kozlov 2000).

## 2.4 *Elastic Properties of the Lipid Membrane*

In the sequel we explore values for the elastic moduli in a lipid bilayer undergoing a traction $\Sigma_M$. Here each pure phase is characterized by a specific value of the stretch $\lambda$, namely $\lambda = \lambda_*$ for the liquid-ordered phase $L_o$ and $\lambda = \lambda^*$ for the liquid-disordered one $L_d$.

**Area compressibility** A tangent area compressibility modulus

$$K_A(\lambda) := \varphi''(\lambda) \tag{45}$$

is defined as the change of surface stress, $\varphi'(\lambda)$, induced by a change in stretch. As the membrane energy $\varphi(\lambda)$ is a fourth-order polynomial, the compressibility stiffness $K_A$ is nonconstant and takes the form

$$K_A(\lambda_*) = K_A(\lambda^*) = 181\,\mathrm{mN\,m^{-1}}, \tag{46}$$

in $\lambda_*$ and $\lambda^*$, and for the unstretched membrane ($\lambda = 1$)

$$K_A(1) = 288\,\mathrm{mN\,m^{-1}}. \tag{47}$$

Henceforth, $K_A$ manifests softening. The obtained values are consistent with measurements available in the literature. In particular, the highest areal stretch is $\delta A/A_0 = \lambda_* - 1 = 0.025$ and it agrees with the value of rupture stretches found in Lipowsky and Sackmann (1995).

**Bending stiffness** Relation $(11)_1$ yields values in agreement with previous results (see e.g., Bermúdez et al. 2004; Evans 1974; Norouzi et al. 2006; Pan et al. 2009; Rawicz et al. 2000). Specifically, in the ordered and disordered phases the following values are obtained:

$$\kappa^{L_o} = \kappa(\lambda_*) = 6.10 \cdot 10^{-19}\,\mathrm{J}, \tag{48}$$

$$\kappa^{L_d} = \kappa(\lambda^*) = 4.78 \cdot 10^{-19}\,\mathrm{J}. \tag{49}$$

It is worth noting that the ratio of these rigidities is

$$\frac{\kappa^{L_o}}{\kappa^{L_d}} = 1.27 \tag{50}$$

in agreement with the experimental findings (see e.g., Baumgart et al. 2003; Semrau et al. 2008).

**Gaussian stiffness** Normally the evaluation of this quantity refers to the spontaneous curvature of each leaflet (Hu et al. 2012; Siegel and Kozlov 2004), while in Deseri and Zurlo (2013), Zurlo (2006) these values are not accounted for. There each leaflet has no spontaneous curvature and the resulting $\kappa_G$ is of the order of $10^{-21}$J. This is then turns out to be two orders of magnitude lower than existing estimates available in Norouzi et al. 2006, Semrau et al. (2008). This discrepancy could be solved either incorporating those spontaneous curvatures of each monolayer of by incorporating the lateral (and highly nonconstant through thickness) pressure profile within the bilayer. This is actually under investigation.

Keeping the approach of Deseri and Zurlo (2013), Zurlo (2006), relations $(9)_2$ and (10) yield

$$\alpha(J) = \frac{k_G(J)}{2J^2}, \tag{51}$$

highlighting the connection between changes of the Gaussian rigidity with changes in the gradient of thinning and, ultimately, of the areal stretch. This connection is actually not surprising. Indeed, thanks to the Gauss–Bonnet Theorem, $k_G$ emerges at the boundaries of each region characterized by constant values of $J$. Namely, $k_G$ appears at the phase boundaries between the $L_o$ and the $L_d$ phases. The role of $\alpha(J)$ emerges instead while trying to evaluate the line tension inside the boundary layer, as highlighted in Sect. 2.3. Such instances are consistent with the relation established in Eq. (51).

## 2.5 The Onset of Change of Elastic Phase

In this section we obtain the linearized equation of lipid membrane under the plane strain geometry (14) with $g_x = \bar{J}$ and $\phi = \bar{\phi}$ (hence $\phi_x = 0$). In this regard let us denote with $\varepsilon$ the strain field perturbing uniformly the stretched configuration just described. The elastic free energy density (20) for the membrane is then evaluated at the perturbed configuration $J = \bar{J} + \varepsilon$, and takes the following form:

$$\begin{aligned}\psi(\varepsilon, \varepsilon_x) &= \varphi\left(\bar{J} + \varepsilon\right) + \alpha(\bar{J} + \varepsilon)||\left(\bar{J} + \varepsilon\right)_x||^2 \\ &\approx \varphi(\bar{J}) + \varphi'(\bar{J})\,\varepsilon + \frac{\varphi''(\bar{J})}{2}\varepsilon^2 + \alpha(\bar{J})\,||\varepsilon_x||^2\,,\end{aligned} \tag{52}$$

where we neglected higher order contributions in $\varepsilon^2$ to define $\psi_{DZ}$. Then the free energy takes the following form:

$$\Psi_{DZ} = \int_\Omega \psi_{DZ}(\varepsilon, \varepsilon_x)dx, \tag{53}$$

where $\Omega \in [-L/2, L/2]$, and

$$\psi_{DZ}(\varepsilon, \varepsilon_x) = \varphi(\bar{J}) + \varphi'(\bar{J})\,\varepsilon + \frac{\varphi''(\bar{J})}{2}\varepsilon^2 + \alpha(\bar{J})\,\varepsilon_x^2\,. \tag{54}$$

The (in-plane) displacement field is expressed through a perturbation $v$ such that $u = \bar{u} + v$, and $\varepsilon(x) = v_x(x)$.

Due to the presence of nonlocal terms $\varepsilon_x$, we recall that the hypertractions $\Gamma$ perform work against displacement gradient $v_x$ at the boundary. Henceforth, the total energy $\mathscr{E}$ change in a neighborhood of the "ground" (homogeneous) configuration reads as follows:

$$\mathscr{E} = B\,\Psi_{DZ} - \mathscr{W}(v, v_x), \tag{55}$$

where the external work reads now as follows:

$$\mathscr{W}(v, v_x) = B\,[\Sigma\ \times\ (\bar{u} + v) + \Gamma\ \times\ (\bar{u}_x + v_x)]_{\partial\Omega}\,, \tag{56}$$

where $\bar{u} = \bar{J}_x$ is zero if the ground configuration is homogeneously stretched. For the sake of conciseness, nonhomogeneous ground configurations will not be analyzed here, although the issue is addressed in Deseri et al. (2016). By substituting (52) and (55) in (56) the total energy change takes the following form:

$$\begin{aligned}\mathscr{E} = B\int_\Omega \left(\varphi + \varphi'(\bar{J})\,v_x + \frac{\varphi''(\bar{J})}{2}v_x^2 + \alpha(\bar{J})\,v_{xx}^2\right)dx \\ - B\,[\Sigma\,v + \Gamma\,v_x]_{\partial\Omega} + \bar{\mathscr{E}},\end{aligned} \tag{57}$$

where

$$\bar{\mathscr{E}} = B \int_\Omega \varphi(\bar{J}) dx - [\Sigma\, \bar{u} + \Gamma\, \bar{u}_x]_{\partial\Omega}\,. \tag{58}$$

From now on, every item with the over-bar is calculated on the ground configuration (e.g., $\bar{\varphi} = \varphi(\bar{J})$ etc.), and we will denote with $'$ the derivative with respect to the spatial variable $x$.

The linear Euler–Lagrange equation for the perturbations of planar membranes is derived through stationarity of $\bar{\mathscr{E}}$ (see Appendix A1 in Deseri et al. 2016 for details). Such equation together with its boundary conditions reads as follows:

$$\begin{cases} 2\bar{\alpha}\, v'''' - \bar{\varphi}''\, v'' = 0 & \text{in } \Omega \\ \text{either } \bar{\varphi}''\, v' - 2\bar{\alpha}\, v''' = \Sigma - \bar{\varphi} \text{ or } \delta v = 0 & \text{in } \partial\Omega \\ \text{either } 2\bar{\alpha}\, v'' = \Gamma \text{ or } \delta v' = 0 & \text{in } \partial\Omega \end{cases} \tag{59}$$

It is worth noting that homogeneous configurations, and hence their corresponding values $\bar{J}$, from which oscillatory perturbations could arise are still not known at this point. In order to find them, a parameter $\omega$ is introduced as follows:

$$\omega^2 := \begin{cases} +\dfrac{\bar{\varphi}''}{2\bar{\alpha}} & \text{if } \bar{\varphi}'' > 0 \\ -\dfrac{\bar{\varphi}''}{2\bar{\alpha}} & \text{if } \bar{\varphi}'' < 0, \end{cases} \tag{60}$$

where, because of (10) and (9), we have

$$\frac{\bar{\varphi}''}{2\bar{\alpha}} = \frac{12}{h_0^2} \frac{\bar{\varphi}''}{\bar{\varphi}'} \bar{J}^5. \tag{61}$$

Relation (59) can then be rewritten as follows:

$$\begin{cases} v'''' \mp w^2\, v'' = 0 & \text{in } \Omega \\ \text{either } \pm\omega^2 v' - v''' = \dfrac{\Sigma - \bar{\varphi}}{2\bar{\alpha}} \text{ or } \delta v = 0 & \text{in } \partial\Omega \\ \text{either } 2\bar{\alpha}\, v'' = \Gamma \text{ or } \delta v' = 0 & \text{in } \partial\Omega. \end{cases} \tag{62}$$

Boundary conditions yield obviously several cases. For the sake of illustration, we choose the case in which the displacement is constrained and the hypertractions are imposed at the boundary, i.e., $v = 0$ and $2\bar{\alpha}\, v'' = \Gamma$.

The value of $\omega^2$ does determine the type of solution arising from this analysis. In particular, the phase changes start to be seen from the onset arising, thanks to the specific value of $\omega^2$. In order to investigate such onset, subcases are identified depending on $\bar{J}$ relative to the landscape of the membrane energy $\varphi$ in Fig. 3. Indeed, because such a function has at most one stationary point $J_0$ unless the lipid bilayer is at its transition temperature, inspection of Fig. 7 below shows that there are four values of $J$ besides $\bar{J}$ to be accounted for, i.e., $J_* \le J_{max} \le J_{min} \le J^*$. Here $J_{max}$

and $J_{min}$ are points of turning curvature for $\varphi(J)$, whereas $J_*$ and $J^*$ are the values of the two points sharing the value of the tangent to the graph of $\varphi(J)$.

Two alternative situations may arise depending on the sign of $\bar{\varphi}''$, depending on whether or not the ground state $\bar{J}$ belongs to the spinoidal, hence unstable, zone of $\varphi(J)$.

## 2.6 Unstable Region: $\bar{\varphi}'' < 0$

The case just mentioned is investigated in this section. Here, $\bar{J}$ is then such that $J_{max} < \bar{J} < J_{min}$, corresponding to a region of negative tangent for the membrane stress $\tau(J) = \varphi'(J)$ (see Fig. 7). The Euler–Lagrange equation (62) takes then the following form:

$$v'''' + \omega^2 v'' = 0, \tag{63}$$

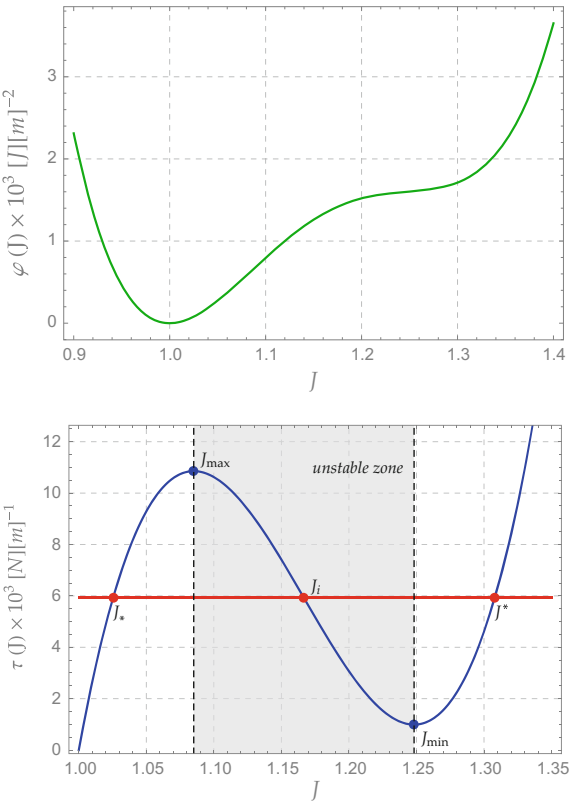


**Fig. 7** The membrane energy $\varphi(J)$ for a temperature $T \sim 30°$ and related local stress $\tau(J)$. The value $J_o = 1$ corresponds to the unstressed, reference configuration $\mathscr{B}_0$ (courtesy of Deseri and Zurlo 2013; Deseri et al. 2016)

which general solution reads as follows:

$$v(x) = A_1 \cos(\omega x) + A_2 \sin(\omega x) + A_3 x + A_4. \tag{64}$$

The primary interest here is to investigate the influence of the boundary conditions below:

$$v\Big|_{\partial\Omega^-} = 0 \qquad v\Big|_{\partial\Omega^+} = 0 \qquad 2\bar{\alpha} v''\Big|_{\partial\Omega^-} = \hat{\Gamma}_L \qquad 2\bar{\alpha} v''\Big|_{\partial\Omega^+} = \hat{\Gamma}_R \tag{65}$$

where $\hat{\Gamma}_R = \Gamma\Big|_{\partial\Omega^+}$ and $\hat{\Gamma}_L = \Gamma\Big|_{\partial\Omega^-}$. For the sake of brevity we set

$$c = \cos(\omega L/2) \quad \text{and} \quad s = \sin(\omega L/2).$$

The boundary conditions assume can be then recast in the following form:

$$\begin{cases} A_1 c - A_2 s - A_3 \dfrac{L}{2} + A_4 = 0 \\ 2\bar{\alpha}\omega^2 (-A_1 c + A_2 s) = \hat{\Gamma}_L \end{cases} \text{at } x = -\frac{L}{2}$$

$$\begin{cases} A_1 c + A_2 s + A_3 \dfrac{L}{2} + A_4 = 0 \\ 2\bar{\alpha}\omega^2 (-A_1 c - A_2 s) = \hat{\Gamma}_R \end{cases} \text{at } x = +\frac{L}{2}$$

We further choose a constant hyperstress at the boundary, namely $\hat{\Gamma}_L = \hat{\Gamma}_R = \hat{\Gamma}$, leading to the simplified set of algebraic conditions below:

$$\begin{bmatrix} 0 & s & \frac{L}{2} & 0 \\ c & 0 & 0 & 1 \\ 0 & s & 0 & 0 \\ -2\bar{\alpha}\,\omega^2 c & 0 & 0 & 0 \end{bmatrix} \begin{pmatrix} A_1 \\ A_2 \\ A_3 \\ A_4 \end{pmatrix} = \begin{pmatrix} 0 \\ 0 \\ 0 \\ \hat{\Gamma} \end{pmatrix}. \tag{66}$$

We record that the determinant of the coefficient matrix of such system reads as follows $\bar{\alpha}\, c\, s\, L\, \omega^2$. We now characterize the nontrivial modes (64) of the system no matter what the value of the hyperstress, namely we investigate the solutions of

$$\bar{\alpha}\, c\, s\, L\, \omega^2 = 0. \tag{67}$$

Because of (10) and $1 < J_{max} < \bar{J} < J_{min}$, we note that $\bar{\alpha} > 0$ for all $\bar{J} > 1$. Then, the orthogonality of the trigonometric functions imposes that the equation is satisfied if either $c = \cos(\omega L/2) = 0$ or $s = \sin(\omega L/2) = 0$.

It follows that we are left to study only two subcases.

**Case 1**. We investigate the case $s = 0$ and $c = \pm 1$. Such instance implies that

$$\omega = \frac{2\, n\, \pi}{L} \tag{68}$$

and relation (68) allows for showing that this circumstance occurs whenever the ground state solves the nonlinear algebraic equation below:

$$\frac{\bar{\varphi}''}{\bar{\varphi}'}\bar{J}^5 = -\frac{n^2\pi^2}{3}\left(\frac{h_0}{L}\right)^2. \tag{69}$$

It is worth noting that the ratio $(h_0/L)^2$ measures the thinness of the bilayer and it is of the order $10^{-8}$ or smaller. Henceforth, from (69) it follows that a large finite number $n$ of oscillations arise in the onset of bifurcation starting from ground states solving (69). Indeed this is possible just by noting that for $J$ such that $\bar{\varphi}'' \to 0^-$, namely right after the change on convexity of $\varphi$. The solution of the resulting system permits to get the amplitudes of the $n^{th}$ mode, i.e.,

$$\begin{bmatrix} 0 & 0 & \frac{L}{2} & 0 \\ \pm 1 & 0 & 0 & 1 \\ 0 & 0 & 0 & 0 \\ \mp 2\bar{\alpha}\,\omega^2 & 0 & 0 & 0 \end{bmatrix} \begin{pmatrix} A_1 \\ A_2 \\ A_3 \\ A_4 \end{pmatrix} = \begin{pmatrix} 0 \\ 0 \\ 0 \\ \hat{\Gamma} \end{pmatrix}$$

then

$$\begin{cases} A_1 = \mp\dfrac{\hat{\Gamma}}{2\bar{\alpha}\,\omega^2} \\ A_3 = 0 \\ A_4 = \mp A_1 \end{cases}.$$

Then, the corresponding buckled solution of order $n$ reads

$$\begin{aligned} v_n(x) = \pm\frac{\hat{\Gamma}}{8\,\bar{\alpha}\,n^2\,\pi^2}\left[\cos\left(2n\pi\frac{x}{L}\right) - 1\right] \\ + A_2 \sin\left(2n\pi\frac{x}{L}\right). \end{aligned} \tag{70}$$

It goes without saying that even if no hyperstress $\hat{\Gamma}$ is present at the boundary, (70) guarantees that a bifurcated mode $v_n = A_2 \sin\left(2n\pi\frac{x}{L}\right)$ does occur.

**Case 2**. We now instead explore the following situation:

$$s = \pm 1 \ \text{ and } \ c = 0.$$

In this case we have

$$\omega = \frac{(1+2\,n)\,\pi}{L} \tag{71}$$

and

$$\frac{\bar{\varphi}''}{\bar{\varphi}'}\bar{J}^5 = -\frac{(1+2n)^2\pi^2}{12}\left(\frac{h_0}{L}\right)^2, \tag{72}$$

which definitely has solutions for $\bar{J}$ so that $\bar{\varphi}'' \to 0^-$ for the same very reason discussed for case 1. Boundary conditions lead to $A_2 = A_3 = A_4 = 0$. It follows that solutions exist if and only if $\hat{\Gamma} = 0$ and they take the form

$$v_n(x) = A_1 \cos(\omega x) = A_1 \cos\left((1+2n)\pi \frac{x}{L}\right). \tag{73}$$

## 2.7 Stability Region: $\bar{\varphi}'' > 0$

If the ground state $\bar{J}$ is not in the spinoidal zone, namely there $\bar{\varphi}'' > 0$, and either $1 < \bar{J} < J_{max}$ or $\bar{J} > J_{min}$, the balance equation reduces to

$$v'''' - \omega^2 v'' = 0, \tag{74}$$

and its general solution becomes

$$v(x) = A_1 \cosh(\omega x) + A_2 \sinh(\omega x) + A_3 x + A_4, \tag{75}$$

hence no oscillations arise.

## 2.8 Singular Ground States: $\bar{\varphi}'' = 0$

Singular values for the ground states are $\bar{J} = J_{max}$ and $\bar{J} = J_{min}$. There, the first derivative of the local stress with respect to $J$ is zero and, hence, $\bar{\varphi}'' = 0$. This immediately tells that $\omega = 0$, and the resulting governing equation, $v'''' = 0$, admits

$$v(x) = A_0 + A_1 x + A_2 x^2 + A_3 x^3 \tag{76}$$

as solution. If (65) are imposed at the boundary with $\hat{\Gamma}_R = \hat{\Gamma}_L = \hat{\Gamma}$, the constants in the previous relation become as follows:

$$A_0 = -\frac{\hat{\Gamma} L^2}{16\bar{\alpha}} \quad A_1 = 0 \quad A_2 = \frac{\hat{\Gamma}}{4\bar{\alpha}} \quad A3 = 0, \tag{77}$$

thereby leading to a unique solution. In other words, no bifurcations arise from singular ground states and perturbations do not arise in the absence of hyperstress at the boundary.

## 3 Hereditariness of Lipid Membranes

Available experimental data Harland et al. (2010), Espinosa et al. (2011), Craiem and Magin (2010) show that lipid bilayers present an *anomalous* rate-dependent behavior within broad ranges of temperature. Anomaly means that if the loss and storage moduli[1] in any rheometric test are plotted against frequency, such quantity scale with a noninteger power of the frequency itself. Indeed, Harland et al. (2010) showed that the storage and loss modulus are proportional to the frequency through a power law of fractional order, i.e., $G^{'}(\omega) \propto \omega^{\beta}$ and $G^{''}(\omega) \propto \omega^{\beta+1}$, where the exponent $\beta$ depends on temperature and specific chemical composition of the biological structure. This justifies the term "fractional" for such a kind of response. Fractional hereditariness is then an intrinsic feature of lipid membranes. Perturbations of the ground states from which bifurcations of phases occur are nucleated and then evolve in time according to such behavior.

Results in Harland et al. (2010) show that lipid membranes are not purely elastic and this is in fact only an asymptotic condition. Nevertheless, such structures have been predominantly modeled as hyperelastic surfaces. Physiological conditions of cells are in fact characterized by intracellular and extracellular viscous fluid compartments cooperating to vary the areal stretch several times during cell lifetimes. The corresponding membrane stress therefore changes in time and can achieve significantly higher values than the ones evaluated by utilizing nonlinear elasticity. The time change of such stress can even evolve to the extent of either causing rupture of the cell membrane or to modify toward ceramide phase, and then to cell apoptosis, the lipids across the membrane (Craiem and Magin 2010).

### *3.1 The Physics of Hereditariness in Lipid Structures*

As pointed out before, lipid systems forming cytoplasmatic membranes present time-hereditary properties (Espinosa et al. 2011). Storage and loss moduli $G^{'}(\omega)$, $G^{''}(\omega)$ of lipid membrane depend on the type of lipids. The presence of very common lipids like phosphatidylcholine (PODC) and sphingomyelin (SM) do heavily influence the rate behavior of lipid layers, thereby showing various morphologies ultimately affecting the resulting effective viscosity of the membrane. The phases can be either liquid-ordered or gel-phase, for temperatures over or below the melting temperatures of the PODC. For SM the liquid-disordered or the solid phase (ceramide) can be involved depending on the temperature of the system.

From the point of view of modeling, it is obvious that the use of Maxwell rheological elements to describe storage and loss moduli of the material does not provide a suitable representation for the behavior of lipid membranes for the simple reason that

[1] For the reader who is not familiar with this standard terminology, we recall that the right-handed Fourier transform of a given relaxation function represents the "complex modulus" of a viscoelastic material; its real part is the "storage modulus", while its imaginary part is its "loss modulus".

Maxwell models yield $G^{'}(\omega) \propto \omega$ and $G^{''}(\omega) \propto \omega^2$, never observed in experiments (see e.g., Espinosa et al. 2011).

It is then obvious that the only way to account for hereditary behavior of lipid membranes must contain fractional-order features, where creep and relaxation are described as power laws so that $J(t) \propto t^{\beta}$ and $G(t) \propto t^{-\beta}$, respectively. Small perturbations arising from homogeneous ground states must then be studied by making use of the Boltzmann–Volterra convolution integral. This allows for keeping track the stress evolution at any $x$ depending on the strain history $\epsilon(x, t)$, namely

$$\sigma(x,t) = \frac{C_\beta}{\Gamma[1-\beta]} \int_{-\infty}^{t} (t-\tau)^{-\beta}\, \dot{\epsilon}(x,\tau)\, d\tau. \tag{78}$$

The right-hand side of the latter relation relates with the Caputo fractional-order derivative $\mathcal{D}_t^{\beta}$ defined as follows:

$$\mathcal{D}_t^{\beta} f(t) = \frac{1}{\Gamma(\beta)} \int_{-\infty}^{t} (t-\tau)^{-\beta} \dot{f}(x,\tau) d\tau, \tag{79}$$

introduced in Caputo (1969) and explored in several papers ever since (see e.g., Podlubny 1998; Magin 2010; Samko et al. 1987; Kilbas et al. 2006). The *springpot element* introduced in Scott-Blair (1974) is a rheological element associated to (79). This detects an intermediate behavior between a linear elastic spring and a viscous dashpot, which are then limiting cases obtained for $\beta = 0$ and $\beta = 1$, respectively.

When it comes to considering more complex studies of nucleations of phase perturbations in the presence of elasticity and viscosity, one needs to provide an expression of the free energy, delivering the key element of a variational principle suitable for the desired investigations. The free energy provided by Deseri et al. (2014) for power law hereditary systems is then used in the sequel. This can be further specialized to characterize the non-dissipated part of the power performed in a given springpot by an underlying stress, thereby allowing for a powerful tool suitable for handling lipid membrane hereditariness.

## 3.2 The Free Energy for Small Perturbations of Planar Lipid Structures

In this section we aim to obtain and solve the balance equations governing the nucleation and evolution of small perturbations of homogeneous ground states in hereditary and planar lipid membranes.

The limiting elastic case is well described through (54), containing both the local term, $\varepsilon(x\, t)$, and a nonlocal one, $\varepsilon_x(x,\ t)$. Henceforth, when it comes to accounting for fractional hereditariness of our systems, the expression of the free energy function is then the sum of contributions related to the local and the nonlocal state variables

(for the notion of state in hereditary systems see e.g., Del Piero and Deseri 1997; Deseri et al. 1999, 2006).

It is then reasonable to infer that nucleation and evolution of small perturbations from homogeneous ground states are determined by the local and nonlocal stresses $\sigma_L(x,t)$ and $\sigma_N(x,t)$ respectively, i.e.,

$$\sigma_L(x,t) = \int_0^t G_L(t-\tau)\dot{\varepsilon}(x,\tau)\,\mathrm{d}\tau, \tag{80a}$$

$$\sigma_N(x,t) = \int_0^t G_N(t-\tau)\dot{\varepsilon}_x(x,\tau)\,\mathrm{d}\tau, \tag{80b}$$

where $G_L$ and $G_N$ represent the local and nonlocal relaxation functions (relative to the given ground state $\bar{J}$), respectively, defined as follows:

$$G_L(t) = \bar{\varphi}'' + f_L(t),$$
$$G_N(t) = 2\bar{\alpha} + f_N(t).$$

Asymptotically, we require the following relations to hold:

$$\lim_{t\to\infty} f_L(t) = \lim_{t\to\infty} f_N(t) = 0, \tag{81}$$

as the elastic case must be retrieved as limit. The analytic dependence of both $f_L(t)$ and $f_N(t)$ on time can be determined by experimental observations of the evolution of the phases as well as of their transition zone. The striking experimental evidence discussed in the section above induces us to utilize a power law relaxation function to model both local and nonlocal evolution of the constitutive response. In general two different laws for describing the local and the nonlocal contributions have to be considered; here we assume

$$G_L(t) = \bar{\varphi}'' + C_L\, t^{-\lambda}, \tag{82a}$$

$$G_N(t) = 2\bar{\alpha} + C_N\, t^{-\nu}, \tag{82b}$$

where $C_L$ and $C_N$ are generalized moduli of the local and nonlocal relaxations, $\lambda$ and $\nu$ are the decay exponents of the relaxations, chosen in the (open) interval $(0, 1)$. Relations (82) yield a fractional-order rheological element introduced in (79).

The free energy function $\Psi(x,\, t)$ is chosen to be additive in two distinguished terms:

$$\Psi(x,\, t) = \Psi_{DZ}(x,\, t) + \Psi_V(x,\, t), \tag{83}$$

where $\Psi_{DZ}(x,\, t)$ is defined by (53) and represents the elastic contribution to the free energy at equilibrium (see Del Piero and Deseri 1996), while $\Psi_V(x,\, t)$ is the free energy characterizing the hereditary response of the system. The latter has been obtained in Deseri et al. (2014). There it has been shown that a multiscale procedure across the spectrum of observation scales of a fractal material does deliver (i) a power

law relaxation function and (ii) a Staverman–Schartzl free energy, which is indeed utilized here for $\Psi_v$. Studies on Staverman–Schartzl free energies can be found in Breuer and Onat (1964), Del Piero and Deseri (1996), Del Piero and Deseri (1997), among other works. The results in Deseri et al. (2014) and formulas (80), (82) yield $\Psi(x,\, t)$ as follows:

$$\Psi(x,\, t) = \Psi_L(\varepsilon(x,\, t)) + \Psi_N(\varepsilon_x(x,\, t)), \tag{84}$$

where the subscripts $L$ and $NL$ stand for local and nonlocal, respectively. The former term depends upon the strain, while the latter one is a functional of its gradient. Results in Breuer and Onat (1964) and Deseri et al. (2014) suggest to introduce a kernel $K(\circ, \circ)$, symmetric in its arguments, namely such that $K(\circ, \circ) \geq 0$ and $K(\tau_1, \tau_2) = K(\tau_2, \tau_1)$ hold. Specifically, each contribution is taken as follows:

$$\begin{aligned}
\Psi_L(x,\, t) &= \frac{1}{2} K_L(0,0)\varepsilon(x,t)^2 \\
&+ \varepsilon(x,t) \int_{-\infty}^{t} \dot{K}_L(0, t-\tau)\varepsilon(x,\tau)\mathrm{d}\tau \\
&+ \frac{1}{2} \int_{-\infty}^{t}\int_{-\infty}^{t} \ddot{K}_L(t-\tau_1, t-\tau_2)\varepsilon(x,\tau_1)\varepsilon(x,\tau_2)\mathrm{d}\tau_1\mathrm{d}\tau_2,
\end{aligned} \tag{85a}$$

$$\begin{aligned}
\Psi_N(x,\, t) &= \frac{1}{2} K_N(0,0)\varepsilon_x(x,t)^2 \\
&+ \varepsilon_x(x,t) \int_{-\infty}^{t} \dot{K}_N(0, t-\tau)\varepsilon_x(x,\tau)\mathrm{d}\tau + \\
&+ \frac{1}{2} \int_{-\infty}^{t}\int_{-\infty}^{t} \ddot{K}_N(t-\tau_1, t-\tau_2)\varepsilon_x(x,\tau_1)\varepsilon_x(x,\tau_2)\mathrm{d}\tau_1\mathrm{d}\tau_2,
\end{aligned} \tag{85b}$$

where

$$K_L(t,0) = \bar{\varphi}'' + \frac{C_L}{\Gamma(1-\lambda)}(t+\delta)^{-\lambda} = G_L^{\delta}(t), \tag{86a}$$

$$K_N(t,0) = 2\bar{\alpha} + \frac{C_N}{\Gamma(1-\nu)}(t+\delta)^{-\nu} = G_N^{\delta}(t), \tag{86b}$$

where $\delta$ is a preloading time. This comes from the fact that no strain process starts with abrupt jump and, instead, it does require some time, $\delta$, to reach a desired value.

The relations $K_L(0,t) = K_L(t,0)$ and $K_N(0,t) = K_N(t,0)$ also do hold. This result, together with (82) and the considerations addressed in Eqs. (17−22) in Deseri et al. (2014), permits to write the free energy as follows:

$$\begin{aligned}\Psi_L(x,\,t) &= \frac{1}{2}G_L^{\delta}(0)\varepsilon^2(x,t)\\ &+ \varepsilon(x,t)\int_{-\infty}^{t}\dot{G}_L^{\delta}(t-\tau)\varepsilon(x,\tau)\mathrm{d}\tau\\ &+ \frac{1}{2}\int_{-\infty}^{t}\int_{-\infty}^{t}\ddot{G}_L^{\delta}(2t-\tau_1-\tau_2)\varepsilon(x,\tau_1)\varepsilon(x,\tau_2)\mathrm{d}\tau_1\mathrm{d}\tau_2,\end{aligned} \tag{87a}$$

$$\begin{aligned}\Psi_N(x,\,t) &= \frac{1}{2}G_N^{\delta}(0)\varepsilon_x^2(x,t)\\ &+ \varepsilon_x(x,t)\int_{-\infty}^{t}\dot{G}_N^{\delta}(t-\tau)\varepsilon_x(x,\tau)\mathrm{d}\tau\\ &+ \frac{1}{2}\int_{-\infty}^{t}\int_{-\infty}^{t}\ddot{G}_N^{\delta}(2t-\tau_1-\tau_2)\varepsilon_x(x,\tau_1)\varepsilon_x(x,\tau_2)\mathrm{d}\tau_1\mathrm{d}\tau_2,\end{aligned} \tag{87b}$$

where $\varepsilon(x,\,t) = v_x(x,\,t)$, and $v(x,\,t)$ is the space-time perturbation process of the underlying ground state of the membrane. Ultimately, the free energy associated with the perturbation process $v(x,t)$ becomes the following:

$$\begin{aligned}\mathscr{E} = B\int_{t_1}^{t_2}\left(\int_{\Omega}\left[\Psi_L(x,\,t)+\Psi_N(x,\,t)\right]\mathrm{d}x\right)\mathrm{d}t\\ - B\,\left[\Sigma\, v(x,t)+\Gamma\, v_x(x,t)\right]_{\partial\Omega},\end{aligned} \tag{88}$$

where $t_1$ and $t_2 > t_1$ are two subsequent times during which the time evolution of the membrane is investigated.

### 3.3 Time Evolution of Phase Perturbations

The governing equation for the evolution of small perturbations $v$ is sought by imposing the stationarity of $\mathscr{E}$ within the class of synchronous variations, i.e., such that $\delta v(\circ, t_1) = \delta v(\circ, t_2)$. This leads to the Euler–Lagrange equation in the following form (see Deseri et al. 2016 for details):

$$2\bar{\alpha}\,\frac{\partial^4}{\partial x^4}\left(v + C_N^{*}\mathcal{D}_t^{\nu}v\right) - \bar{\varphi}''\,\frac{\partial^2}{\partial x^2}\left(v + C_L^{*}\mathcal{D}_t^{\lambda}v\right) = y(x), \tag{89}$$

where $C_L^{*} = C_L/\bar{\varphi}''$ and $C_N^{*} = C_N/2\bar{\alpha}$ represent the normalized local and nonlocal moduli of the membrane, respectively, and the forcing term $y(x)$ is defined as follows:

$$y(x) = 2\bar{\alpha}\frac{\partial^4 v_0}{\partial x^4} - \bar{\varphi}''\frac{\partial^2 v_0}{\partial x^2}, \tag{90}$$

where $v_0(x)$ is an initial perturbation induced on the system. This represents the initial perturbation of the ground state before the relaxation takes place. The balance

equation (89) is endowed with the boundary conditions to be retrieved from the following conditions:

$$\begin{cases} \text{either} \\ \bar{\varphi}'' \left(v' + \bar{C}_L \mathcal{D}_t^{\lambda} v'\right) - 2\bar{\alpha} \left(v''' + \bar{C}_N \mathcal{D}_t^{\nu} v'''\right) = \Sigma + \Sigma_0 \\ \text{or} \\ \delta v = 0 \end{cases} \tag{91a}$$

$$\begin{cases} \text{either} \\ 2\bar{\alpha} \left(v'' + \bar{C}_N \mathcal{D}_t^{\nu} v''\right) = \Gamma + 2\bar{\alpha}\, \varepsilon_0' \\ \text{or} \\ \delta v' = 0 \end{cases} \tag{91b}$$

Here $\Sigma_0 = \bar{\varphi}'' \varepsilon_0 + 2\,\bar{\alpha}\, \varepsilon_0''$ is the initial stress arising on the bilayer associated with the initially perturbed configuration. Obviously, whenever the membrane is initially perturbation-free then (89) and its boundary conditions give us an eigenvalue problem: this will be solved in Sect. 3.6.

Separation of variables is employed here to solve (89), namely we seek for solutions in the form

$$v(x,t) = f(x)\, q(t), \tag{92}$$

where $q(t)$ describes the time change of the perturbation and $f(x)$ describes the shape of the mode. Substitution of (92) in (89) leads to the following pair of equations

$$\frac{2\bar{\alpha}}{\bar{\varphi}''} \frac{f''''(x)}{f''(x)} = \frac{q(t) + C_L^* \mathcal{D}_t^{\lambda} q(t)}{q(t) + C_N^* \mathcal{D}_t^{\nu} q(t)} = k^2, \tag{93}$$

where $k^2$ is a constant to be determined. We remind that the expression (60) relating $\frac{2\bar{\alpha}}{\bar{\varphi}''}$ to the spatial frequency (squared) $\omega^2$ does hold. Because here we focus on the circumstances for which spatial oscillations can occur, the only case of interest is when $\bar{\varphi}'' < 0$. Henceforth, we will solve the following equations:

$$-\frac{1}{\omega^2} \frac{f''''(x)}{f''(x)} = \frac{q(t) + C_L^* \mathcal{D}_t^{\lambda} q(t)}{q(t) + C_N^* \mathcal{D}_t^{\nu} q(t)} = k^2. \tag{94}$$

The very same boundary conditions assumed for the elastic case (65) will be considered for the viscoelastic problem, namely:

$$\begin{cases} v\Big|_{\partial\Omega^-} = v\Big|_{\partial\Omega^+} = 0 \\ 2\bar{\alpha} \left[v'' + C_N^* \mathcal{D}_t^{\nu} v''\right]\Big|_{\partial\Omega^-} = 2\bar{\alpha} \left[v'' + C_N^* \mathcal{D}_t^{\nu} v''\right]\Big|_{\partial\Omega^+} = \hat{\Gamma} \end{cases} \tag{95}$$

which by (92) yield the following relations:

$$\begin{cases} f(x)\Big|_{\partial\Omega} = 0 \\ 2\bar{\alpha} f'' \left[q(t) + C_N^* \mathcal{D}_t^\nu q(t)\right]\Big|_{\partial\Omega} = \hat{\Gamma} \end{cases} \tag{96}$$

### 3.4 Spatial Modes for the Perturbations

The spatial mode $f(x)$ verifies (93), namely

$$f''''(x) + k^2 \omega^2 f''(x) = 0. \tag{97}$$

the solution of (97) reads as

$$f(x) = A_1 \cos(\zeta x) + A_2 \sin(\zeta x) + A_3 x + A_4, \tag{98}$$

after setting

$$\zeta^2 = k^2 \omega^2 . \tag{99}$$

Boundary conditions (96) allow for determining the coefficients $A_i$, $i = 1 \div 4$. In particular, the second boundary condition yields

$$2\bar{\alpha} f''\Big|_{\partial\Omega}\left[q(t) + C_N^* \mathcal{D}_t^\nu q(t)\right] = \hat{\Gamma} \qquad \forall t,$$

to be satisfied if either $\hat{\Gamma}$ is a prescribed function of time or if it is constant. Whenever this is the case, then

$$q(t) + C_N^* \mathcal{D}_t^\nu q(t) = \kappa_n, \tag{100}$$

where $\kappa_n$ is a constant. Consequently, the boundary condition under exam reads as follows:

$$2\bar{\alpha} f''\Big|_{\partial\Omega} \kappa_n = \hat{\Gamma}. \tag{101}$$

Moreover, this condition at the edge highlights that the second derivative evaluated in such location $v"(x, t)\Big|_{\partial\Omega}$ can be zero for whatever value of $\kappa_n$ if and only if no hyperstress arises at the edges, i.e.,

$$f''\Big|_{\partial\Omega} = 0 \iff \hat{\Gamma} = 0. \tag{102}$$

For such a case, Eq. (100) is irrelevant. After setting $s = \sin(\zeta L/2)$ and $c = \cos(\zeta L/2)$, the boundary conditions can be written explicitly in the following form:

$$\begin{cases} A_1\, c - A_2\, s - A_3 \dfrac{L}{2} + A_4 = 0 \\ 2\bar{\alpha}\zeta^2\,(-A_1\, c + A_2\, s)\,\kappa_n = \hat{\Gamma} \end{cases} \text{at } x = -\frac{L}{2}$$

$$\begin{cases} A_1\, c + A_2\, s + A_3 \dfrac{L}{2} + A_4 = 0 \\ 2\bar{\alpha}\zeta^2\,(-A_1\, c - A_2\, s)\,\kappa_n = \hat{\Gamma} \end{cases} \text{at } x = +\frac{L}{2}$$

Such a system is the analog of (66):

$$\begin{bmatrix} 0 & s & \frac{L}{2} & 0 \\ c & 0 & 0 & 1 \\ 0 & s & 0 & 0 \\ -2\bar{\alpha}\,\kappa_n\zeta^2 c & 0 & 0 & 0 \end{bmatrix} \begin{pmatrix} A_1 \\ A_2 \\ A_3 \\ A_4 \end{pmatrix} = \begin{pmatrix} 0 \\ 0 \\ 0 \\ \hat{\Gamma} \end{pmatrix} \tag{103}$$

whose nontrivial solutions can be found by studying the roots of the determinant, namely after solving:

$$\bar{\alpha}\, c\, s\, L\, \kappa_n\, \zeta^2 = 0. \tag{104}$$

The ground states $\bar{J}$ from which bifurcations may occur are given by the latter equation no matter what $\kappa_n$, and because the constants $\bar{\alpha}$, $L$ are always nonzero, only two possibilities are left.

**Case 1**. Because $\zeta^2 = k^2\,\omega^2$ with $k > 0$ (although still unknown at this stage), if $s = 0$ we have

$$k^2\,\omega^2 = \frac{4n^2\pi^2}{L^2}, \tag{105}$$

and

$$-\frac{\bar{\varphi}''}{\bar{\varphi}'}\,\bar{J}^5 = \frac{n^2\pi^2}{3\,k^2}\left(\frac{h_0}{L}\right)^2. \tag{106}$$

**Case 2**. If $c = 0$ then $\hat{\Gamma} = 0$. As highlighted in (102), this happens if and only if $f''\,(\partial\Omega) = 0$.

### *3.5 Time Evolutions of the Perturbations*

The expression of $q(t)$ can be traced back to the solution of the equation coming from the boundary condition (101).

Whenever in (96) the boundary condition on the second derivative of the displacement is nonzero, the presence of a hyperstress $\hat{\Gamma}$ at the edges implies that the time-dependent term is constant, assuring that relation (100) holds. This equation is solved in Deseri et al. (2016) and delivers the following expression:

$$q(t) = \frac{\kappa_n}{C_N^*} t^\nu E_{\nu,\nu+1}\left(-\frac{1}{C_N^*} t^\nu\right) + q_0 E_\nu\left(-\frac{1}{C_N^*} t^\nu\right), \tag{107}$$

where $E_{\alpha,\beta}(z)$ is the Mittag-Leffler function of two parameters.

Nonetheless, separation of variables imposes (93) to be fulfilled. This, together with relation (100), delivers the following differential equation:

$$q(t) + C_L^* \mathcal{D}_t^\lambda q(t) = k^2 \kappa_n, \tag{108}$$

again solved in Deseri et al. (2016) by means of the same method, delivering the following expression for $q$:

$$q(t) = \frac{k^2 \kappa_n}{C_L^*} t^\lambda E_{\lambda,\lambda+1}\left(-\frac{1}{C_L^*} t^\lambda\right) + h_0 E_\lambda\left(-\frac{1}{C_L^*} t^\lambda\right). \tag{109}$$

Obviously the two obtained expressions for $q$ must agree at all times. This is certainly true in the trivial case for which the local and nonlocal terms have both the same relaxation exponent $\lambda = \nu$ and the same normalized parameters $C_L^* = -C_N^*$, namely $k^2 = 1$, recalling that $C_L^* < 0$ has been rendered nondimensional by taking $C_L$ and dividing it by $\bar{\varphi}'' < 0$.

### 3.6 *Eigenvalue Problem Governing the Time Dependence of the Perturbations*

Because Eqs. (93) and (100) both govern the evolution function $q$ a complete study of such a requirement is needed. Indeed, those two equations deliver the following fractional-order eigenvalue problem:

$$C_L^* \mathcal{D}_t^\lambda q(t) - C_N^* k^2 \mathcal{D}_t^\nu q(t) + (1 - k^2) q(t) = 0. \tag{110}$$

The solution method of such a problem is here based on the right-sided Fourier transform $Q(p)$

$$Q(p) := \int_0^{+\infty} e^{-i\,p\,t} q(t)\, dt \qquad p \in \mathbb{R}. \tag{111}$$

By Fourier transforming both sides of (110) we obtain

$$\left[C_L^* (-i\,p)^\lambda - C_N^* k^2 (-i\,p)^\nu + (1 - k^2)\right] Q(p) = 0. \tag{112}$$

The zeros of the function inside square brackets provide the eigenvalues of the fractional differential equation (110) no matter what $Q(p)$ is. It is worth noting that the constant $k^2$ appearing in (93) for the first time must be a real number. The algebraic equation (112) can actually be manipulated by separating the real and the imaginary parts as follows:

$$k^2 = \frac{1 + C_L^* \, p^\lambda \, (c_\lambda - i \, s_\lambda)}{1 + C_N^* \, p^\nu \, (c_\nu - i \, s_\nu)}$$
$$= \frac{\left(1 + C_L^* \, p^\lambda \, c_\lambda\right) - i \, \left(C_L^* \, p^\lambda \, s_\lambda\right)}{\left(1 + C_N^* \, p^\nu \, c_\nu\right) - i \, \left(C_N^* \, p^\nu \, s_\nu\right)} = \frac{a - i \, b}{c - i \, d}$$
$$= \frac{a - i \, b}{c - i \, d} \frac{c + i \, d}{c + i \, d} = \frac{a \, c + b \, d}{c^2 + d^2} + i \frac{a \, d - b \, c}{c^2 + d^2},$$

after setting

$$\begin{cases} a = 1 + C_L^* \, p^\lambda \, c_\lambda \\ b = C_L^* \, p^\lambda \, s_\lambda \end{cases} \qquad \begin{cases} c = 1 + C_N^* \, p^\nu \, c_\nu \\ d = C_N^* \, p^\nu \, s_\nu \end{cases},$$

$$c_\alpha = \cos(\alpha \, \pi/2)$$

$$s_\alpha = \sin(\alpha \, \pi/2),$$

$\alpha = \lambda, \, \nu$. Because $k$ is real, the former complex algebraic equation delivers the following real-valued conditions to be verified, namely,

$$k^2 = \frac{a \, c + b \, d}{c^2 + d^2} \tag{113a}$$
$$a \, d - b \, c = 0. \tag{113b}$$

Equation (113b) can be rewritten as follows:

$$C_N^* \, p^\nu \, s_\nu - C_L^* \, p^\lambda \, s_\lambda + C_L^* \, C_N^* \, p^{\lambda+\nu} \, (s_\nu c_\lambda - c_\nu s_\lambda) = 0$$

and, through the transformation formulas for the difference of two angles, it becomes

$$C_N^* \, p^\nu \, \sin\left(\nu \, \frac{\pi}{2}\right) - C_L^* \, p^\lambda \, \sin\left(\lambda \, \frac{\pi}{2}\right) + \\ + C_L^* \, C_N^* \, p^{\lambda+\nu} \sin\left((\nu - \lambda) \, \frac{\pi}{2}\right) = 0. \tag{114}$$

Finally, a relationship for $k^2$ is found in the following form:

$$k^2 = \frac{\left(1 + C_L^* \, p^\lambda \, c_\lambda\right) \left(1 + C_N^* \, p^\nu \, c_\nu\right) + \left(C_L^* \, p^\lambda \, s_\lambda\right) \left(C_N^* \, p^\nu \, s_\nu\right)}{\left(1 + C_N^* \, p^\nu \, c_\nu\right)^2 + \left(C_N^* \, p^\nu \, s_\nu\right)^2}. \tag{115}$$

Whenever the trivial case $\lambda = \nu$ and $C_L^* = C_N^*$ is considered, Eq. (114) has solution $p = 0$, that implies $k^2 = 1$, as noticed qualitatively above. The solution of (115) cannot be found in closed form. In Figs. 8 and 9 some numerical results are represented whenever the moduli $C_L^*$, $C_N^*$ and both the exponents are known.

The ratio

$$R = -C_L^* / C_N^*$$

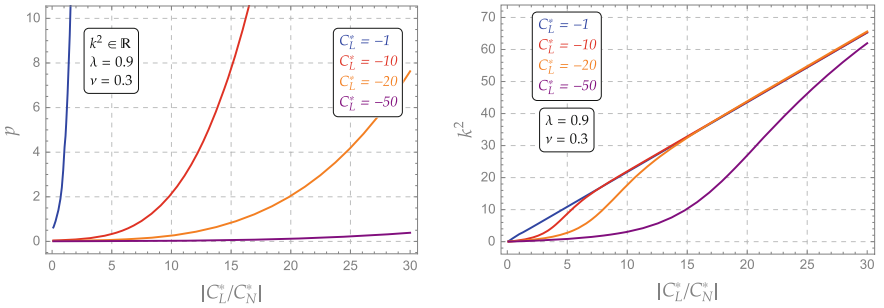


**Fig. 8** Locus of the real values of $p$ and correspondent eigenvalues $k^2$ as function of the ratio $R = -C_N^*/C_L^*$ whenever $\lambda = 0.9$ and $\nu = 0.3$ (see (114) and (115)) (courtesy of Deseri et al. 2016)

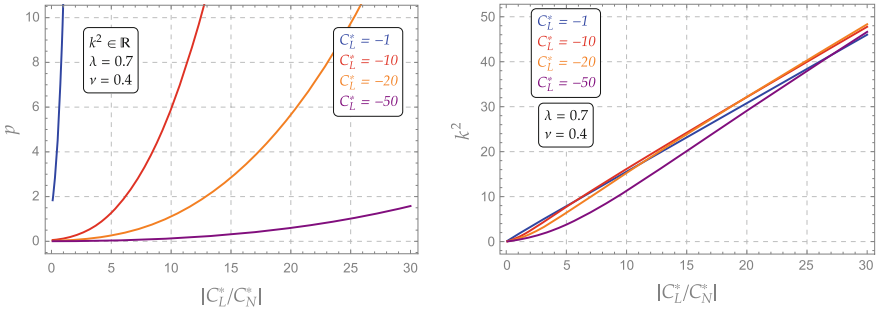


**Fig. 9** Locus of the real values of $p$ and correspondent eigenvalues $k^2$ as function of the ratio $R = -C_N^*/C_L^*$ whenever $\lambda = 0.7$ and $\nu = 0.4$ (see (114) and (115)) (courtesy of Deseri et al. 2016)

shows that the eigenvalues are bijections of $p$. Hence, there is also a one-to-one correspondence between $R$ and $k^2$. Of course, each bifurcation is characterized by a value of $k^2$ which modifies the left and right branch of the ratio $\bar{\varphi}''/\bar{\varphi}'$:

$$-k^2 \frac{\bar{\varphi}''}{\bar{\varphi}'} \bar{J}^5 = \frac{n^2\pi^2}{3} \left(\frac{h_0}{L}\right)^2, \tag{116}$$

which is the viscoelastic analog of (69).

A numerical example based on the very same energetics utilized in the elastic case is displayed in Fig. 10. This diagram shows that $k^2$ acts as a rescaling parameter, thereby amplifying the ratio $\bar{\varphi}''/\bar{\varphi}'$ as $k$ increases. While the values of $J_n$ are not modified by such rescaling, the upper bound of the curve is highly influenced by such parameter. This has an impact on the maximum number of oscillations, $n_{max}$, as displayed in Fig. 10. Henceforth, by plotting in Fig. 11 the values of the critical $J$ in terms of the number of oscillations, one can notice that the left (blue color) and right (red color) branches do have different shapes, thereby modifying their intersections with any given $\bar{J}$.

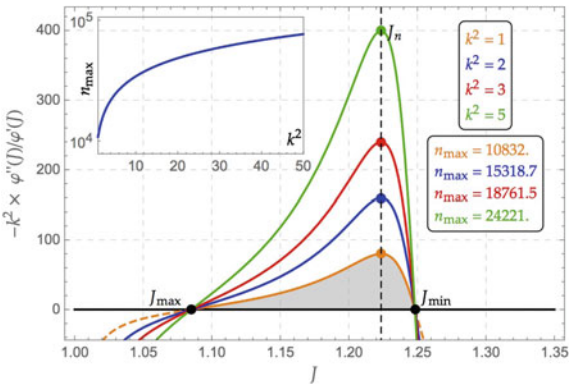


**Fig. 10** Left-hand side of Eq. (116) in terms of $J$. It is highlighted the influence of of $k^2$ and the corresponding maximum number of spatial oscillations $n_{max}$ is displayed (courtesy of Deseri et al. 2016)

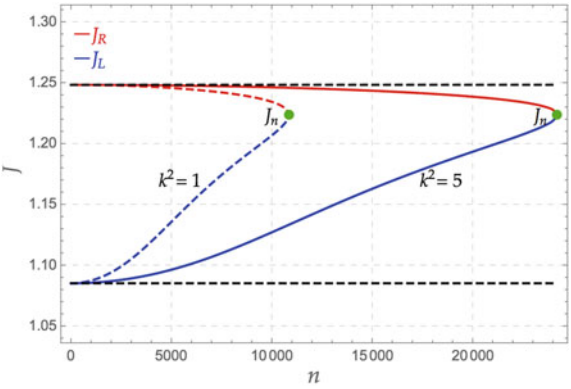


**Fig. 11** Modification of the left and right intersections depending on $k^2$ (courtesy of Deseri et al. 2016)

## 3.7 *Influence of the Initial Conditions*

The "full" fractional differential equation (110) with inhomogeneous initial conditions is analyzed in this section, namely,

$$\begin{cases} C_L^* \mathcal{D}_t^{\lambda} q(t) - C_N^* k \mathcal{D}_t^{\nu} q(t) + (1 - k^2) q(t) = 0, \\ q(0) = q_0. \end{cases}$$

The right-handed Fourier transform is again employed here to account the initial condition, i.e.,

$$C_L^* \left[ (i\, p)^{\lambda} \hat{Q} - (i\, p)^{\lambda - 1} q_0 \right] - C_N^* k^2 \left[ (i\, p)^{\nu} \hat{Q} + \right.$$
$$\left. - (i\, p)^{\nu - 1} q_0 \right] + \hat{Q}\,(1 - k^2) = 0,$$

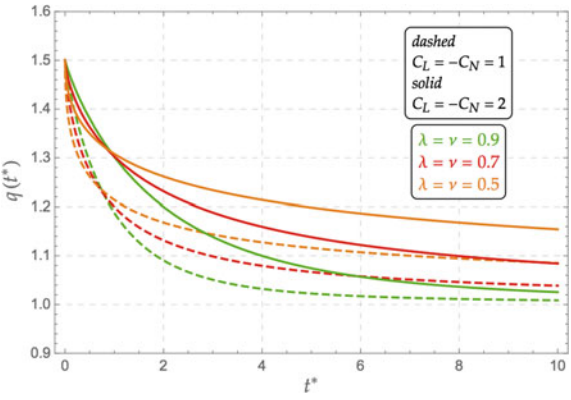


**Fig. 12** Time-dependent transfer function for two chosen values of $C_L^* = -C_N^*$ and $h_0 = 1.5$. Here $t^* = \sqrt[\nu]{\frac{t^\nu}{C_N^*}}$ is a dimensionless time (courtesy of Deseri et al. 2016)

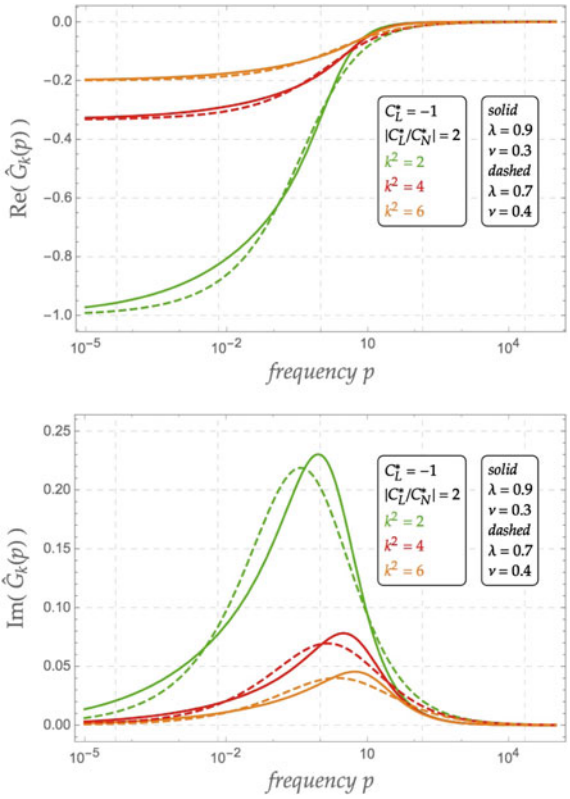


**Fig. 13** Transfer function $\hat{G}_k(p)$: real and imaginary parts (courtesy of Deseri et al. 2016)

whose solution $\hat{Q}(p)$ reads as follows:

$$\hat{Q}_k(p) = \hat{G}_k(p)\, q_0 \left( C_L^* (i\ p)^{\lambda-1} - C_N^* k^2 (i\ p)^{\nu-1} \right), \tag{117}$$

where

$$\hat{G}_k(p) = \frac{1}{C_L^* (i\ p)^{\lambda} - C_N^* k^2 (i\ p)^{\nu} + (1-k^2)} \tag{118}$$

is the transfer function for this problem. It is worth noting that this function strictly depends on the order of the eigenvalue, $k^2$.

From Podlubny (1998), Eqs. 5.22–5.25, p. 155 (where $a = C_L^*$, $\beta = \lambda$, $b = -C_N^* k^2$, $\alpha = \nu$ and $c = 1 - k^2$), we find the anti-right-handed Fourier transform of such a function, which reads as follows:

$$\begin{aligned} G_k(t) &= \mathcal{F}^{-1}\left\{ \hat{G}_k(p); t \right\} = \\ &= \frac{1}{C_L^*} \sum_{z=0}^{\infty} (-1)^z \left( \frac{1-k^2}{C_L^*} \right)^{z+1} t^{\lambda(z+1)-1} E^{(z)}_{\lambda-\nu,\lambda+z\nu}\left( \frac{C_N^*}{C_L^*} k^2\, t^{\lambda-\nu} \right). \end{aligned} \tag{119}$$

The obtained result is then represented by a series of Mittag-Leffler functions with two parameters. This plays the role of modulating the membrane response no matter what the initial data is. For the sake of illustration, the transfer function is numerically explored in Fig. 12 whenever two subcases of $C_L^* = -C_N^*$ are considered, by assuming several values of the exponential decay $\lambda = \nu$. Similarly, in Fig. 13 the real and imaginary parts of the transfer function are analyzed whenever different exponents of the decay $\lambda \neq \nu$ are chosen for some values of $k^2$. The Mittag-Leffler function drives the evolution of the membrane stretch, determining changes in the amplitude of the membrane response, as expected from the analysis with a separation of variables.

## 4 Conclusions

The mechanical behavior of biological membranes is regulated by the interaction of an extremely rich list of features, such as their thinness, their special constitutive nature which enables them to sustain bending moments but not in-plane shear stresses unless their viscosity is accounted for, their chemical composition and, furthermore, their capability of undergoing ordering–disordering phenomena. The resulting effects of this interaction are evidenced by a strong variety of configurations that can be achieved and kept by biological membranes at equilibrium for given values of overall chemical composition, controlled temperature, or applied osmotic pressure.

Within this framework, a remarkable issue is the analysis of line tension at the boundary of ordered–disordered domains: it is now recognized that, together with bending rigidities, line tension plays a major role in maintaining nonspherical configurations observed in experiments (see e.g., Akimov et al. 2004). In the effort of

deducing a physically based model of lipid membranes where the bending behavior, the order–disorder transition, and the chemical composition are consistently considered, in Deseri et al. (2008), Deseri and Zurlo (2013), Zurlo (2006) the expression of the energetics regulating the thermo-chemo-mechanical behavior of biological membranes was derived, within the framework of a formal asymptotic 3D-to-2D reduction, based on thinness assumptions. This model reveals the possibility of describing the geometrical (shape) and conformational (state of order) behavior of the lipid bilayer on the basis of one single ingredient: the in-plane membrane stretching elasticity, regulating the material response with respect to local area changes on the membrane mid-surface. A confirmation of these possibilities is given in Choksi et al. (2012), where a model energy obtainable from the one deduced in Deseri et al. (2008) is proved to exhibit two-phase global minimizers resembling observed configurations in Baumgart et al. (2003). In essence, the major point in Deseri et al. (2008), Deseri and Zurlo (2013), Zurlo (2006) is that the bilayer stretching elasticity is enough to describe its order–disorder transition (together with the influence of chemical composition), to determine the profile and the length of the boundary layer where the membrane thickness passes from a thicker domain (ordered phase) to a thinner one (disordered phase), to evaluate the corresponding line tension and finally to determine the bending rigidities in both phases.

A prototypical planar problem has been studied in Deseri and Zurlo (2013) with the aim of elucidating the potentials of the model described above and summarized in the present work. On the basis of a Landau expansion of the stretching energy density, calibrated, thanks to the experimental results in Goldstein and Leibler (1989), the line tension, the thickness profile inside the boundary layer and the area compressibility and bending moduli are obtained. Those calculated quantities show a satisfactory comparison with the data known in the literature.

Lipid phase transition arising in planar membrane and triggered by material instabilities and their linearized evolution are studied in Deseri et al. (2016) and summarized in this work. There, the effective viscoelastic behavior inherited by their exhibited power law in-plane viscosity (Espinosa et al. 2011) is accounted for. At first it is shown that the critical set of areal stretches is determined in the limiting case of elasticity and for two sets of boundary conditions. Spatial oscillations corresponding to the nucleated configurations arising from any of such critical stretches are investigated. Perturbations of the phase ordering of lipids are predicted to form bifurcated shapes, sometimes of large periods relative to the reference thickness of the bilayer. The corresponding membrane stress changes are also oscillatory. Then, the influence of the effective viscoelasticity of the membrane on its material instabilities is investigated. A variational principle based on the search of stationary points of a Gibbs free energy in the class of synchronous perturbation is employed for such analysis. The resulting Euler–Lagrange equation is a fractional-order partial differential equation yielding a non-classical eigenvalue initial boundary value problem. The eigenvalues are found to be amplified with respect to their elastic counterpart. Spatial modes and transfer functions characterizing the resulting admissible perturbations of the underlying ground configurations are determined. It is found that while the range of critical areal stretches not get affected, the number of oscillations per given critical

stretch significantly increases, thereby drastically reducing the period of oscillations of the bifurcated configurations. Nevertheless, a "long tail" type relaxation of the bifurcated configurations is shown to occur. Furthermore, whenever the same power law applies both for the local and the nonlocal response, the explicit time decay is displayed, while in all of the other cases the frequency dependence of the real and imaginary parts of the transfer function reveal that fading memory in time occurs as well (see Fig. 13).

**Acknowledgements** The author wishes to thank the organizer of this course, David Steigmann, for his invitation to contribute to this course. The other lecturers are also acknowledged for the nice and extended discussions that allowed for exchange of ideas on the topic of this course.

The author is extremely grateful to Giuseppe Zurlo (National University of Galway, Ireland), formerly his Ph.D. student, for the very extensive discussions and long-standing collaboration from his early days in 2002. His key contribution to this research has had huge impact in its assessment and development. Timothy J. Healey (Cornell University) and Roberto Paroni (University of Sassari, Italy) also gratefully acknowledged for the very extended discussions on the early stages of the 2008 work.

Grateful acknowledgements go to Massimiliano Zingales (University of Palermo), Kaushik Dayal (Carnegie Mellon University) as collaborators on key aspects related to the hereditary response of lipid bilayers. Massimiliano Fraldi (University of Napoli-Federico II) is also gratefully ackowledged for his illuminating remarks and insights on biological tissues and biomechanics, as well as Valentina Piccolo (University of Trento), a graduate student working with myself and other people on various topics, who also provided new perspectives on the applications of Fractional Analysis to lipid membranes and helped a lot to edit this work.

The author is grateful to the financial support provided by (i) the NSF Grant no.DMS-0635983 of the Center for Nonlinear Analysis, Carnegie Mellon University, (ii) for the direct financial support of the Dept. of Mechanical Engineering and Materials Science-MEMS of the University of Pittsburgh for, and also to (iii) the support of the EU Grant "INSTABILITIES" ERC-2013-ADG Instabilities and nonlocal multiscale modelling of materials held by Prof. Davide Bigoni from the University of Trento.

## References

S.A. Akimov, P.I. Kuzmin, J. Zimmerberg, An elastic theory for line tension at a boundary separating two lipid monolayer regions of different thickness. J. Electroanal. Chem. **564**, 13–18 (2004)

G. Alberti, An approach via $\Gamma-$convergence, in *Calculus of Variations and Partial Differential Equations*, Topics on Geometrical Evolution Problems and Degree Theory, ed. by L. Ambrosio, N. Dancer (Springer, Berlin, 2000)

E. Baesu, R.E. Rudd, J. Belak, M. McElfresh, Continuum modeling of cell membranes. Int. J. Non-Linear Mech. **39**(3), 369–377 (2004)

T. Baumgart, W.W. Webb, S.T. Hess, Imaging coexisting domains in biomembrane models coupling curvature and line tension. Nature **423**, 821–824 (2003)

H. Bermúdez, D.A. Hammer, D.E. Discher, Effect of bilayer thickness on membrane bending rigidity. Langmuir **20**, 540–543 (2004)

S. Breuer, E. Onat, On the determination of free energies in linear viscoelastic solids. ZAMP **15**, 184–191 (1964)

J.W. Cahn, J.E. Hilliard, Free energy of a non-uniform system i - interfacial free energy. J. Chem. Phys. **28**, 258–267 (1958)

P.B. Canham, The minimum energy as possible explanation of the biconcave shape of the human red blood cell. J. Theor. Biol. **26**(1), 61–81 (1970)
M. Caputo, *Elasticità e Dissipazione* (Zanichelli, Bologna, 1969)
R. Choksi, M. Morandotti, M. Veneroni, Global Minimizers for Axisymmetric Multiphase Membranes, arXiv preprint (2012), arXiv:1204.6673
B.D. Coleman, D.C. Newman, On the rheology of cold drawing. i. elastic materials. J. Polym. Sci.: Part B: Polym. Phys. **26**, 1801–1822 (1988)
D. Craiem, R.L. Magin, Fractional order models of viscoelasticity as an alternative in the analysis of red blood cell (rbc) membrane mechanics. Phys. Biol. **7**(1), 13001 (2010)
G. Del Piero, L. Deseri, On the analytic expression of the free energy in linear viscoelasticity. J. Elast. **43**, 247–278 (1996)
G. Del Piero, L. Deseri, On the concepts of state and free energy in linear viscoelasticity. Arch. Ration. Mech. Anal. **138**, 1–35 (1997)
L. Deseri, G. Zurlo, The stretching elasticity of biomembranes determines their line tension and bending rigidity. Biomech. Model. Mechanobiol. **12**, 1233–1242 (2013)
L. Deseri, G. Gentili, M.J. Golden, An expression for the minimal free energy in linear viscoelasticity. J. Elast. **54**, 141–185 (1999)
L. Deseri, M.J. Golden, M. Fabrizio, The concept of a minimal state in viscoelasticity: new free energies and applications to pdes. Arch. Ration. Mech. Anal. **181**, 43–96 (2006)
L. Deseri, M. Piccioni, G. Zurlo, Derivation of a new free energy for biological membranes. Contin. Mech. Term **20**(5), 255–273 (2008)
L. Deseri, M. Di Paola, M. Zingales, Free energy and states of fractional-order hereditariness. Int. J. Solids Struct. **51**, 3156–3167 (2014)
L. Deseri, P. Pollaci, M. Zingales, K. Dayal, Fractional hereditariness of lipid membranes: Instabilities and linearized evolution. J. Mech. Behav. Biomed. Mater. **58**, 11–27 (2016)
G. Espinosa, I. López-Montero, F. Monroy, D. Langevin, Shear rheology of lipid monolayers and insights on membrane fluidity. PNAS **108**(15), 6008–6013 (2011)
E.A. Evans, Bending resistance and chemically induced moments in membrane bilayers. Biophys. J. **14**, 923–931 (1974)
M.S. Falkovitz, M. Seul, H.L. Frisch, H.M. McConnell, Theory of periodic structures in lipid bilayer membranes. Proc. Natl. Acad. Sci. USA **79**, 3918–3921 (1982)
Y.C. Fung, Theoretical considerations of the elasticity of red blood cells and small blood vessels. Proc. Fed. Am. Soc. Exp. Biol. **25**(6), 1761–1772 (1966)
Y.C. Fung, P. Tong, Theory of sphering of red blood cells. Biophys. J. **8**, 175–198 (1968)
R.E. Goldstein, S. Leibler, Model for lamellar phases of interacting lipid membranes. Phys. Rev. Let. **61**(19), 2213–2216 (1988)
R.E. Goldstein, S. Leibler, Structural phase transitions of interacting membranes. Phys. Rev. A. **40**(2) (1989)
M. Hamm, M.M. Kozlov, Elastic energy of tilt and bending of fluid membranes. Eur. Phys. J. E **3**, 323–335 (2000)
C.W. Harland, M.J. Bradley, R. Parthasarathy, Phospholipid bilayers are viscoelastic. PNAS **107**(45), 19146–19150 (2010)
T.J. Healey, R. Paroni, L. Deseri, Material gamma-limits for biological in-plane fluid plates. (2017)
W. Helfrich, Elastic properties of lipid bilayers: theory and possible experiments. Z. Naturforsch [C], **28**(11), 693–703 (1973)
M. Hu, J.J. Briguglio, M. Deserno, Determining the gaussian curvature modulus of lipid membranes in simulations. Biophys. J. **102**, 1403–1410 (2012)
F. Jahnig, Critical effects from lipid-protein interaction in membranes. Biophys. J. **36**, 329–345 (1981)
F. Jahnig, What is the surface tension of a lipid bilayer membrane? Biophys. J. **71**, 1348–1349 (1996)
J.B. Keller, G.J. Merchant, Flexural rigidity of a liquid surface. J. Stat. Phys. **63**(5–6), 1039–1051 (1991)

A.A. Kilbas, H.M. Srivastava, J.J. Trujillo, *Theory and Applications of Fractional Differential Equations* (Elsevier, Amsterdam, 2006)
W.T. Koiter, On the nonlinear theory of thin elastic shells. Proc. K. Ned. Akad. Wet. B **69**, 1–54 (1966)
S. Komura, H. Shirotori, P.D. Olmsted, D. Andelman. Lateral phase separation in mixtures of lipids and cholesterol. Europhys. Lett. **67**(2) (2004)
R. Lipowsky, E. Sackmann (eds.), *Handbook of Biological Physics-Structure and Dynamics of Membranes*, vol. 1 (Elsevier Science B.V, Amsterdam, 1995)
R.L. Magin, Fractional calculus models of complex dynamics in biological tissues. Comput. Math. Appl. **59**(5), 1586–1593 (2010)
M. Maleki, B. Seguin, E. Fried, Kinematics, material symmetry, and energy densities for lipid bilayers with spontaneous curvature. Biomech. Model. Mechanobiol. **12**(5), 997–1017 (2013)
D. Norouzi, M.M. Müller, M. Deserno, How to determine local elastic properties of lipid bilayer membranes from atomic-force-microscope measurements: a theoretical analysis. Phys. Rev. E, **74** (2006)
J.C. Owicki, H.M. McConnell, Theory of protein-lipid and protein-protein interactions in bilayer membranes. Proc. Natl. Acad. Sci. USA **76**, 4750–4754 (1979)
J.C. Owicki, M.W. Springgate, H.M. McConnell, Theoretical study of protein-lipid interactions in bilayer membranes. Proc. Natl. Acad. Sci. USA **75**, 1616–1619 (1978)
J. Pan, S. Tristram-Nagle, J.F. Nagle, Effect of cholesterol on structural and mechanical properties of membranes depends on lipid chain saturation. Phys. Rev. E: Stat. Nonlinear **80**(021931) (2009)
I. Podlubny, *Fractional Differential Equation* (Academic, New York, 1998)
W. Rawicz, K.C. Olbrich, T. McIntosh, D. Needham, E. Evans, Effect of chain length and unsaturation on elasticity of lipid bilayers. Biophys. J. **79**, 328–339 (2000)
A.S. Reddy, D. Toledo Warshaviak, M. Chachisvilis, Effect of membrane tension on the physical properties of dopc lipid bilayer membrane. Bioch. Biophys. Acta **1818**, 2271–2281 (2012)
S.G. Samko, A.A. Kilbas, O.I. Marichev, *Fractional Integrals and Derivatives. Theory and Applications* (Gordon & Breach Science Publishers, London, 1987)
G.W. Scott-Blair, Psychoreology: links between the past and the present. J. Texture Stud. **5**, 3–12 (1974)
S. Semrau, T. Idema, L. Holtzer, T. Schmict, C. Storm, Accurate determination of elastic parameters for multicomponent membranes. PRL **100**(088101) (2008)
D.P. Siegel, M.M. Kozlov, The gaussian curvature elastic modulus of n-monomethylated dioleoylphosphatidylethanolamine: Relevance to membrane fusion and lipid phase behavior. Biophys. J. **87**, 366–374 (2004)
D.J. Steigmann, Fluid films with curvature elasticity. Arch. Ration. Mech. Anal. **150**, 127–152 (1999)
M. Trejo, M. Ben, Amar. Effective line tension and contact angles between membrane domains in biphasic vesicles. Eur. Phys. J. E **34**(8), 2–14 (2011)
S.L. Veatch, V.I. Polozov, K. Gawrisch, S.L. Keller, Liquid domains in vescicles investigated by nmr and fluorescence microscopy. Biophys. J. **86**, 2910–2922 (2004)
G. Zurlo. Material and geometric phase transitions in biological membranes. Dissertation for the Fulfillment of the Doctorate of Philosophy in Structural Engineering, University of Pisa, etd-11142006-173408 (2006)

http://www.springer.com/978-3-319-56347-3

The Role of Mechanics in the Study of Lipid Bilayers

Steigmann, D.J. (Ed.)
2018, VII, 332 p. 72 illus., 30 illus. in color., Hardcover
ISBN: 978-3-319-56347-3